12-2011

The Dissociation Of Location And Object Working Memory Using Fmri And Meg

Antony Passaro

THE DISSOCIATION OF LOCATION AND OBJECT WORKING MEMORY

USING FMRI AND MEG

By

Antony Passaro, B.A.

APPROVED:

_____
Andrew Papanicolaou, Ph.D.
Supervisory Professor

_____
Anthony Wright, Ph.D.

_____
Anne Sereno, Ph.D.

_____
Khader Hasan, Ph.D.

_____
Ponnada Narayana, Ph.D.

APPROVED:

_____
George Stancel, Ph.D., Dean, The University of Texas
Health Science Center at Houston
Graduate School of Biomedical Sciences

THE DISSOCIATION OF LOCATION AND OBJECT WORKING MEMORY USING FMRI AND MEG

A DISSERTATION

Presented to the Faculty of

The University of Texas

Health Science Center at Houston

and

The University of Texas

M. D. Anderson Cancer Center

Graduate School of Biomedical Sciences

in Partial Fulfillment

of the Requirements

for the Degree of

DOCTOR OF PHILOSOPHY

by

Antony Damian Passaro, BA

Houston, Texas

December, 2011

DEDICATION

To my parents who always pushed me to do better and work harder. Your encouragement and support gave me the confidence to accomplish all that I have today. To my friends and family who have supported me with the utmost encouragement and patience.

ACKNOWLEDGMENTS

First and foremost, I would like to thank my mentors, Dr. Andrew Papanicolaou and Dr. Anthony Wright, for their unwavering guidance and encouragement from the moment we first met. They provided me with the knowledge, support, and tools I needed to accomplish my goals.

I would like to thank everyone in both Dr. Wright's Lab and Dr. Papanicolaou's Lab for all of their support, especially Dr. Roozbeh Rezaie for his insight and advice. Thanks to Dr. Timothy Ellmore for all of our talks about fMRI and Dr. Eduardo Castillo and Dr. Joshua Breier for all of our talks about MEG. Through everyone's support, I never stopped learning and things always seemed to get easier.

I would also like to thank Dr. Anne Sereno, Dr. Khader Hasan, and Dr. Ponnada Narayana for their guidance and suggestions as members of my supervisory committee.

THE DISSOCIATION OF LOCATION AND OBJECT WORKING MEMORY USING FMRI AND MEG

Publication No.

Antony Passaro

Supervisory Professor: Andrew Papanicolaou, Ph.D.

Visual working memory (VWM) involves maintaining and processing visual information, often for the purpose of making immediate decisions. Neuroimaging experiments of VWM provide evidence in support of a neural system mainly involving a fronto-parietal neuronal network, but the role of specific brain areas is less clear. A proposal that has recently generated considerable debate suggests that a dissociation of object and location VWM occurs within the prefrontal cortex, in dorsal and ventral regions, respectively. However, re-examination of the relevant literature presents a more robust distribution suggestive of a general caudal-rostral dissociation from occipital and parietal structures, caudally, to prefrontal regions, rostrally, corresponding to location and object memory, respectively.

The purpose of the present study was to identify a dissociation of location and object VWM across two imaging methods (magnetoencephalography, MEG, and functional magnetic imaging, fMRI). These two techniques provide complimentary results due the high temporal resolution of MEG and the high spatial resolution of fMRI. The use of identical location and object change detection tasks was employed across techniques and reported for the first time.

Moreover, this study is the first to use matched stimulus displays across location and object VWM conditions.

The results from these two imaging methods provided convergent evidence of a location and object VWM dissociation favoring a general caudal-rostral rather than the more common prefrontal dorsal-ventral view. Moreover, neural activity across techniques was correlated with behavioral performance for the first time and provided convergent results. This novel approach of combining imaging tools to study memory resulted in robust evidence suggesting a novel interpretation of location and object memory. Accordingly, this study presents a novel context within which to explore the neural substrates of WM across imaging techniques and populations.

TABLE OF CONTENTS

LIST OF FIGURES

LIST OF FIGURES

LIST OF TABLES

LIST OF ABBREVIATIONS

AC……..Anterior Cingulate

Area PG…….Parietal Area G

Area TE……..Temporal Area

Ba……..Brodmann Area

CD…….Change Detection

CEN……Central Executive Network

CUN…….Cuneus

DICS……Dynamic Imaging of Coherent Sources

DLPFC……Dorsolateral Prefrontal Cortex

ECD…….Equivalent Current Dipole

EEG……Electroencephalography

EPI……...Echo Planar Image

ERD……Event-Related Desynchronization

ERF……Event-Related Field

ERS……Event-Related Synchronization

FEF…….Frontal Eye Field

FFA……Fusiform Face Area

fMRI……..Functional Magnetic Resonance Imaging

FUS……Fusiform Gyrus

ICA…….Independent Component Analysis

IFG……...Inferior Frontal Gyrus

IPL…….Inferior Parietal Lobule

IPS…….Inferior Parietal Sulcus

ITG……..Inferior Temporal Gyrus

ITI……..Inter-Trial Interval

LOC……..Lateral Occipital Gyrus

MEG……Magnetoencephalography

MFG…….Middle Frontal Gyrus

MNI……..Montreal Neurological Institute

MOG……..Middle Occipital Gyrus

PCUN…….Precuneus

PET…….Positron Emission Topography

Pre-SMA……Pre-Supplementary Motor Area

SFS……..Superior Frontal Sulcus

SPL…….Superior Parietal Lobule

STG……..Superior Temporal Gyrus

TE……...Echo Time

TF…….Time-Frequency

TR……..Repetition Time

VLPFC……Ventrolateral Prefrontal Cortex

VSTM……Visual Short-Term Memory

VWM……...Visual Working Memory

WM……..Working Memory

CHAPTER 1

INTRODUCTION

1.1 Background

The ability to retain visual information in memory over brief time periods is necessary for accomplishing daily goal-directed tasks. Most often, the duration of retention required for accomplishing these tasks is short and it is referred to as visual short-term memory (VSTM). One empirically established approach for studying VSTM is through a change detection (CD) paradigm, which tests for the memory of visual objects by: (1) the presentation of a stimulus display of objects, (2) followed by a delay, and (3) a test display with a changed object. The CD paradigm allows for the adjustment of task parameters such as stimulus duration, delay time, item complexity, and the type of information (for example, identities of objects vs. their locations) to study VSTM. In the following sections, we review the basic aspects of brief visual memory, including efforts to outline its neural substrates.

In 1974, Baddeley and Hitch differentiated between the concept of VSTM and that of visual working memory (VWM). According to them, in addition to encoding and maintenance, VWM involves the mental manipulation of information held in VSTM. VWM is a limited capacity system in that only a restricted amount of information may be maintained and manipulated as is the case in processing linguistic information, mental calculation, or matching a mental representation to a visual stimulus, which is the essence of the CD paradigm. On the basis of deficits observed in clinical populations, the neuronal basis of VWM appears to be composed of constituent parts. Previous studies of VWM have found significant deficits among patients across a wide range of

disorders affecting different brain regions, including Alzheimer's disease, Parkinson's disease, multiple sclerosis, schizophrenia, Huntington's disease, and dyslexia (e.g., Baddeley et al., 1986; Lange et al., 1995; Litvan et al., 1988; Morris et al., 1988; Park & Holzman, 1992; Rutkowski et al., 2003). Further support for the notion that VWM consists of different operations, each associated with different brain mechanisms, comes from studies of patients with selective lesions in the frontal, temporal, and parietal lobes (e.g., Frisk & Milner, 1990; Owen et al., 1990; Pisella et al., 2004).

Neuroimaging studies of VWM have primarily focused on imaging the brain during the maintenance period during which visual information is maintained in mind. Generally, findings from research involving a variety of VWM tasks (including CD) have identified a network of brain regions comprised of the lateral prefrontal and parietal cortices bilaterally (e.g., Cabeza and Nyberg, 2000; Cohen et al., 1997; Courtney et al., 1997; D'Esposito et al., 1998; Haxby et al., 2000; Linden et al., 2003; Mottaghy et al., 2003; Munk et al., 2002; Pessoa et al., 2002; Postle and D'Esposito, 1999; Postle et al., 2000; Smith & Jonides, 1998). This fronto-parietal network, termed the central executive network (CEN) (Seeley et al. 2007), plays a central role in VWM, although it is posited that parietal regions also play a role in memory capacity (e.g., Todd & Marois, 2004; Vogel & Machizawa, 2004) while additional prefrontal regions likely play a more executive role in the organization of visual information (e.g., Curtis & D'Esposito, 2003; Levy & Goldman-Rakic, 2000). However, the degree to which components of this network are further separable has yet to be elucidated. Importantly, it remains

unclear whether the maintenance involved in this network processes different aspects of visual information, that is, object identities versus object locations.

The distinction of cortical systems specific to the encoding of locations and object identities was initially described by Ungerleider and Mishkin (1982) on the basis of findings from neuroanatomical and behavioral experiments in monkeys. Subsequently, studies using monkeys described the two systems as divergent pathways, the one involving occipito-temporal regions constituting the ventral stream or the “what” pathway responsible for visual object identities and the other, involving the occipito-parietal regions as the dorsal stream or the “where” pathway, responsible for processing the location of visual objects (e.g., Ettlinger, 1990; Livingstone & Hubel, 1987; Mishkin et al., 1983). Studies from human patients seem to support this separation. For example, a patient with agnosia (patient D.F.) sustained lesions in occipito-temporal areas bilaterally and was shown to have deficits in object perception but intact location processing (Milner et al., 1991). The convergent evidence from both human and non-human primate studies was later confirmed by human brain mapping studies using functional magnetic resonance imaging (fMRI) and positron emission tomography (PET), which identified analogous neuroanatomical correlates of location and object identity perception in the parietal and temporal cortices, respectively (e.g. Allison et al., 1994; Haxby et al., 1991; Sergent et al., 1992). Taken together, the aforementioned findings revealed neural substrates that dissociate visual information processing concerning location and object identity at an early stage of stimulus processing following the visual input.

In monkeys, the dorsal pathway was shown to extend from Area PG (parietal area PG, caudal part of the inferior parietal lobule) to dorsolateral prefrontal areas while the ventral path extends from Area TE (temporal area, caudal part of the inferotemporal cortex) to ventrolateral prefrontal regions (Macko et al., 1982). Subsequent lesion studies using non-human primates provided concordant evidence for this dorsal-ventral separation of pathways in the prefrontal cortex (Bachevalier & Mishkin, 1986; Desimone & Ungerleider, 1989). Human studies do not afford the same level of focal sensitivity due to the investigator's inability to induce permanent lesions, which may explain why the extension of these two pathways to specific prefrontal regions in humans has yet to be established.

What can be said about the human neural correlates in regards to object and location VWM? The concept of a domain-specific separation of VWM on the basis of the information (object or location) remembered dates back to the late 20th century. In an attempt to establish a domain-specific segregation of pathways in VWM similar to that described by for perceptual encoding Ungerleider and Mishkin's (1982), fMRI and PET studies sought to identify a dorsal-ventral separation of pathways for location and object identity memory within the prefrontal cortex involving the ventrolateral prefrontal cortex (VLPFC), the dorsolateral prefrontal cortex (DLPFC), and other prefrontal regions (e.g., Courtney et al., 1998; Smith et al., 1996). Additionally, an alternative model suggested the existence of a left-right dissociation extending across the entire brain, which was associated with WM for object identities and locations,

respectively (e.g., D'Esposito et al., 1998; Smith et al., 1995). Several meta-analyses provided evidence in favor of both views (Cabeza & Nyberg, 2000; Courtney et al., 1998; Levy and Goldman-Rakic, 2000; Owen, 2000), thus ultimately failing to provide unequivocal support for the one view over the other. Specifically, some early neuroimaging experiments generated results favoring a dorsal-ventral domain-specific separation in the prefrontal cortex (e.g., Courtney et al., 1996; Jonides et al., 1993), while others reported results which were not in agreement with this separation (e.g., Duncan & Owen 2000; Owen et al., 1999). As a result of such conflicting findings, the dorsal-ventral separation within the prefrontal cortex was de-emphasized in later studies, which involved post-hoc analysis of prefrontal dorsal-ventral structures (e.g., Mohr et al., 2006; Sala et al., 2003). Most fMRI and PET studies which claimed a dorsal-ventral separation in the prefrontal cortex focused on only one or two regions dorsally, corresponding to location memory, and only one or two regions ventrally, corresponding to object identity memory. But there is variability in the specific regions responsible for these two different aspects of VWM. For example, memories for object identities were shown to involve Brodmann area 10 (Ba 10) of the inferior frontal gyrus (IFG) in one instance (e.g., Mohr et al., 2006) and Brodmann area 46 (Ba 46) of the middle frontal gyrus (MFG) in another (e.g., Sala et al., 2003). This divergence in findings may in part be attributable to differences in task design and cognitive requirements across studies, though, within each independent study, task differences are minimal with specific task demands typically corresponding to object memory or location memory only (e.g., Harrison et al.,

2010; Sala & Courtney, 2007). Therefore, the divergence of the findings in favor of a prefrontal dorsal-ventral dissociation in addition to those studies which report conflicting results suggests that a spatially defined prefrontal dorsal-ventral dissociation for location and object identity memory may likely not exist. In fact, a reexamination of the relevant studies suggests that more rostral regions, primarily within the prefrontal cortex, were associated with object identity memory while more caudal regions extending from occipital and parietal regions to posterior frontal regions were associated with location memory. Importantly, a meta-analysis of early PET and fMRI studies of VWM and attention/perception by Ungerleider (1995) actually suggests a general caudal-rostral dissociation independent of the prefrontal dorsal-ventral one outlined by the author. More recent fMRI studies focusing on location and object identity memory using simple objects or pictures implicate a similar caudal-rostral interpretation (Borowsky et al., 2005; Harrison et al., 2010; Mohr et al., 2006; Sala & Courtney, 2007; Sala et al., 2003). Moreover, a study by Leung and Alain (2011) of auditory working memory in the context of location and object identity resulted in findings which coincide with a caudal-rostral distinction of location and object identity working memory, suggesting that this functional gradient in the brain may extend across sensory modalities. **Figure 1.1** illustrates both the prefrontal dorsal-ventral view (**A**) and the proposed general caudal-rostral view (**B**) of location and object VWM dissociation.

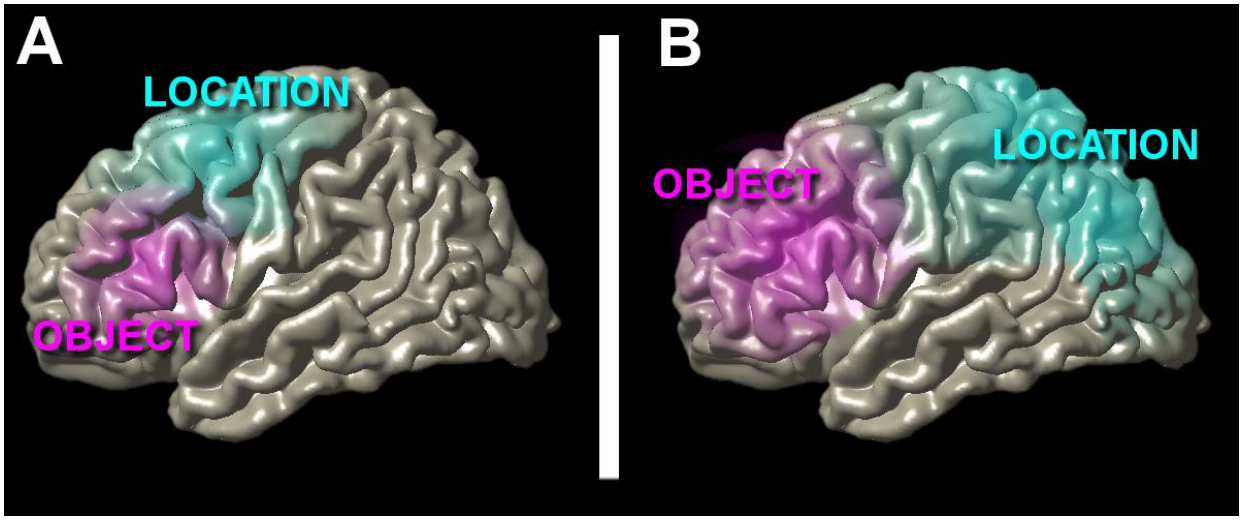

Figure 1.1 Views of domain-specific VWM dissociation

An illustration of two separate views of location and object identity dissociation. **A**. Prefrontal dorsal-ventral view of dissociation corresponding to location and object identity memory, respectively. **B.** General caudal-rostral view of dissociation corresponding to location and object identity memory, respectively.

Though a preponderance of functional imaging studies support a prefrontal dorsal-ventral separation, findings vary by hemisphere and by the anatomical extent of activation within the prefrontal cortex. Generally, a more consistent interpretation of location and object identity VWM across studies suggests that more caudal structures such as the middle occipital gyrus (MOG), the inferior parietal lobule (IPL), superior parietal lobule (SPL), Brodmann area 40 (Ba 40), and even some posterior frontal structures such as the frontal eye field (FEF), and the superior frontal sulcus (SFS) are associated with location memory. Conversely, rostral areas in the prefrontal cortex, such as Brodmann area 10 (Ba 10), Brodmann area 44 (Ba 44), Brodmann area 46 (Ba 46), and Brodmann area 9 (Ba 9) in the inferior and middle frontal gyri appear to be associated with object memory (**Figure 1B**). These associations are examined in studies during the delay period when no visual stimulus is present and visual information is maintained in mind. Accordingly, brain regions associated with the

primary visual response are typically not reported when comparing location and object identity VWM.

While empirical evidence suggests that location or object identity memory are subserved by distinct brain regions, there is likely overlap across these two types of cognitive operations in all or most of the regions identified. For example, a brain region implicated in the maintenance of object memory may also play a role in the processing of location memory, but perhaps to a lesser degree. This point of clarification is critical when discussing dissociable brain regions based on function. Indeed, overlap in function may be assessed on the basis of several parameters, including the time of regional engagement, or intensity of regional activation, in response to an exogenous stimulus. Especially when one considers the spatial and temporal imprecision and general noise associated with imaging techniques, it is unlikely that an all-or-nothing association between function and brain region exists, particularly within the context of object and location WM. With regards to the nature of items in space, it is impossible to completely dissociate the two fundamental properties which all visual items share, namely an item's location and its' identity. These two components are necessary in order to separate one item from the next during simultaneous presentation. As such, it is not surprising that imaging studies report spatially overlapping regions of activation (irrespective of activation amplitude) associated with both location and object identity memory. While it has been shown that visual information is encoded in separate dorsal-ventral streams on the basis of object identities or locations, it is unlikely that information pertaining to the opposing stream is not

processed concurrently, even at relatively low activation levels. Therefore, within a caudal-rostral interpretation of location-object VWM, it is likely that there will exist some regional overlap for object identity memory, namely within caudal regions (e.g., MOG, IPL, SPL). Similarly, some activation corresponding to location memory may be observed in more rostral regions (e.g., Ba 44, 46, 9, 10). This is in agreement with several fMRI studies which report time-course plots demonstrating significant activation for both object and location memory across caudal and rostral regions (Harrison et al., 2010; Mohr et al., 2006; Sala & Courtney, 2007; Sala et al., 2003).

To make direct comparisons between a location memory condition and an object identity memory condition, the use of identical visual displays across conditions is necessary, which is reported here for the first time. Moreover, only a few studies have combined location and object identity memory requirements within a single condition when attempting to dissociate the neural correlates of these two types of memories (Sala & Courtney, 2007; Harrison et al., 2010). By testing for maintenance specific to locations or object identities in the context of a third condition, which directly combines these two aspects, an effect of condition may be studied. Specifically, Sala and Courtney (2007) used object and location trials as well as a combination of the two (*AND* condition) and found that the hemodynamic response associated with the *AND* condition varied across time in various prefrontal regions but remained in-between the activation levels for the object condition and the location condition. This finding suggests a split-resource model of object and location memory and showed how the amount of domain-

specific information was combined across conditions. This condition and approach was used in the experiments reported here to aid in disambiguating the neural correlates associated with location and object identity memory.

1.2 Objectives & Hypotheses

The overarching goal of the work presented in this dissertation is to identify a caudal-rostral framework of location and object identity VWM by examining VWM in the context of a CD task with two imaging modalities, fMRI and magnetoencephalography (MEG). This was done by addressing three key objectives:

1) To verify the dissociation of location and object identity VWM.

2) To provide convergent evidence from two complementary imaging methods on location and object identity VWM for the first time.

3) To determine if a general caudal-rostral dissociation of location and object identity memory exists in contrast to a prefrontal dorsal-ventral dissociation.

To explore and demonstrate these dissociations, four different CD conditions were tested and directly compared within each imaging method. Importantly, only the delay period between stimulus displays was considered as that period corresponds to VWM operations. One of the four VWM conditions was an object-change condition and another condition was a location-change

condition with trial-matched displays across both conditions. A third condition referred to as an *OR* condition required subjects to remember both objects and locations and also used trial-matched displays identical to those used in the object and location change conditions. Finally, a fourth condition referred to as a *location only* condition required subjects to remember object locations while reducing the object information by using a single color within individual trials. It is possible to include the exact same unique stimulus displays across all conditions such that a direct comparison of a trial unique configuration between the conditions would yield a result based unequivocally on the occurred change. Importantly, this approach of matched stimulus displays across conditions is described for the first time and reported here.

1.3 Dissertation Organization

In **Chapter 2**, the neural correlates associated with each condition mentioned above were described using fMRI. A simple multiple regression analysis of the hemodynamic response was employed to analyze each condition prior to comparing conditions directly. Main effects of task condition were identified and reported.

In **Chapter 3**, an approach similar to chapter 2 was utilized for all four conditions and described using MEG. A distributed source spatial filter (beamformer) was applied to the theta range (3-9 Hz) of the MEG signal to localize brain activity associated with each condition. A direct comparison of all

four conditions was used to identify a distributed network of object and location memory.

Finally, in **Chapter 4**, memory performance correlated with brain activity derived by MEG and fMRI was described. These results show functional significance of critical brain regions and present a comparison of behaviorally correlated memory activity across these two imaging techniques reported here for the first time.

CHAPTER 2

UTILIZING FMRI TO STUDY OBJECT AND LOCATION MEMORY

2.1 INTRODUCTION

The VWM literature utilizing fMRI and PET has attempted to establish a model of dissociation corresponding to VWM for locations and object identities. Several early human PET studies have reported a functional dissociation between location and object identity memory (e.g., Courtney et al., 1996; Kohler et al., 1998; Moscovitch et al., 1995). Similarly, a domain-based segregation has also been reported in early fMRI studies (e.g., McCarthy et al., 1996; Petrides et al., 1993). The majority of these studies explored spatial and object memory under the influence of the original findings of Mishkin and Ungerleider (1982), which suggested a prefrontal dorsal-ventral location-object separation. Based on work with monkeys using single-unit recordings and lesion methods, it has been shown that both dorsal and ventral regions within the prefrontal cortex respond to location and object memory respectively (Funahashi et al., 1989; Funahashi et al., 1993; Petrides, 1995; Rushwroth et al., 1997). However, other studies employing similar techniques with monkeys have found contrary results (Levy & Goldman-Rakic, 1999; Passingham, 1985).

An early review of the WM literature by Levy and Goldman-Rakic (2000) suggested domain-specific differences existed within the prefrontal cortex corresponding to the maintenance of spatial and object information. While no definite conclusions were drawn, it was suggested that each domain (location and object) was separable within the prefrontal cortex. Later, a meta-analysis by Wager and Smith (2003) of 60 fMRI and PET studies on WM found no evidence in favor of a dissociation between dorsolateral and ventrolateral prefrontal

regions corresponding to location and object memory. In fact, the authors report that spatial storage was more commonly associated with peak activations in Ba 46, while object storage was more commonly associated with peak activity in the right dorsolateral Ba 9. This finding conflicts with an earlier meta-analysis by Cabeza and Nyberg (2000) which included approximately 70 PET and fMRI studies on WM. However, a re-examination of the findings by Cabeza and Nyberg suggests another interpretation of location-object dissociation for WM: the peak values of spatial memory tasks are typically located in more caudal regions in the brain (occipital, parietal, and posterior frontal regions) while peak values for identity memory tasks are clustered rostrally in prefrontal regions. The same caudal-rostral interpretation is apparent in the meta-analysis by Wager and Smith (2003), although these authors did not pursue this possibility.

The proposed caudal-rostral interpretation for location and object memory dissociation has not been actively pursued by any group to the best of our knowledge. Because the proposed domain-specific framework corresponds to a preponderance of findings across studies, the boundaries of dissociation corresponding to location and object identity memories are unclear. Among the three meta-analyses described above, the majority of the studies reviewed illustrate a preponderance of peak activation sites in favor of spatial memory extending from occipital lobe regions to parietal regions including a frontal lobe region near Ba 6 and the posterior portion of the superior frontal sulcus (SFS). Conversely, there is a prevalence of peak activation sites corresponding to object memory in more rostral regions extending from Ba 10 to slightly more posterior

frontal regions in Ba 46 and the inferior portion of Ba 9 spreading to Ba 6. Should a location-object VWM dissociation exist within a general caudal-rostral framework as identified from meta-analyses, then a well-controlled for VWM experiment (like the one proposed here) should be able to identify such a dissociation.

Across fMRI studies of VWM, several focal brain regions have been consistently implicated in either location or object identity memory. Specifically, the DLPFC in the left hemisphere has been shown to correspond to object memory in comparison to location memory among a broad range of fMRI studies on VWM (e.g., Courtney et al., 1996; Mohr et al., 2006; Sala et al., 2003; Sala & Courtney, 2007; Smith & Jonides, 1999). Similarly, the inferior parietal lobule (IPL) appears to support location memory in comparison to object memory across the same studies. Hemispheric laterality, however, associated with findings of location memory in this region has not been consistent across studies. Several studies have also implicated the SFS (what is likely the FEF) as a location memory brain region (Borowsky et al., 2005; Harrison et al., 2010; Sala et al., 2003; Sala & Courtney, 2007). Dissociations observed within these regions coincide with a caudal-rostral interpretation of location and object identity VWM. Specifically, the IPL is a caudal region with greater activity for location memory, and the DLPFC is a rostral region with greater activity for object identity memory. Therefore, we hypothesize that a caudal-rostral framework will explain the functional dissociation observed among location and object identity memory

conditions in this experiment.

2.2 MATERIALS & METHODS

Subjects

Fifteen healthy subjects (seven men, 23-33 years old) participated in the study and provided written informed consent and were compensated financially for their time. Ten subjects participated in each of the four conditions. Study procedures were approved by the University of Texas Health Science Center at Houston Institutional Review Board. All subjects were in good health with no history of psychiatric or neurological disease and had normal or corrected-to-normal (with contact lenses) visual acuity.

Task

The stimulus set across conditions included nine colored squares (red, blue, green, yellow, orange, pink, purple, teal, and lime green). Each stimulus subtended a visual angle of 1.3 degrees. Six stimuli were displayed on a black background in 6 locations from an invisible grid of 16 possible locations. By remembering the configuration associated with the empty space in a given stimulus display (termed the empty-space strategy) rather than the individual items presented, it is possible to provide an unfair advantage pertaining to location change conditions. To prevent empty-space strategies from occurring during location change conditions, an invisible location grid was created using 2 invisible concentric circles, each with 8 possible locations equally spaced around

the circle. During the fMRI scans, stimuli were displayed on a screen that was mounted behind the subject's head, outside of the scanner. The image was reflected from a mirror onto a small screen directly above the subject's eyes for a viewing angle of 36.0 degrees.

Subjects were tested in 4 change detection conditions: object change detection requiring the subject to remember the color of each square (*object condition*), location change detection (*location condition*), object and location change detection with the subject unaware as to which property of the square would change (*or condition*), and location change detection with a uniform color across items (*location only condition*) (**Figure 2.1**). Due to the number of trials and the overall length for each condition, subjects participated in two conditions per fMRI scan such that the *object condition* and the *location condition* were grouped together in a single session and the *or condition* and the *location only condition* were grouped in another session. The use of matched stimulus displays across conditions employed in this experiment has not been previously reported within the neuroimaging literature on VWM.

Within each session, individual conditions were blocked and subjects were verbally informed about the condition prior to the start of each block. Subjects completed 10 alternating blocks of 23 trials (5 *object* and 5 *location* or 5 *or* and 5 *location only* depending on the session) for a total of 230 trials and 115 trials per condition. In all conditions, trials began with a variable 4 or 6-s fixation period. During the fixation period, a small white fixation cross (1.8 degrees of visual angle) was presented in the middle of a black background. Following fixation, the

sample period began. During this period, six colored squares were presented on the screen simultaneously for 2 seconds. Next, there was a 2 second delay period with an empty black display. The test period followed with two colored squares presented, one remained the same relative to the sample display but one had changed in either color (*object condition*), location (*location condition*), color or location (*or condition*), or location with all squares a single color (*location only condition*). Subjects were instructed to covertly decide which square had changed. Finally, during the response period, a white box was randomly presented around one of the two colored squares (boxed item). During the response period subjects made a yes/no response using a fiber-optic response pad (Current Designs, Philadelphia) to indicate whether or not the boxed item had changed. The motor response was separated from the test display to prevent contamination from motor-related activity. Following the response period, the inter-trial interval (ITI) began, which consisted of either 4 or 6-s of passive fixation to allow for a temporal jitter across trials.

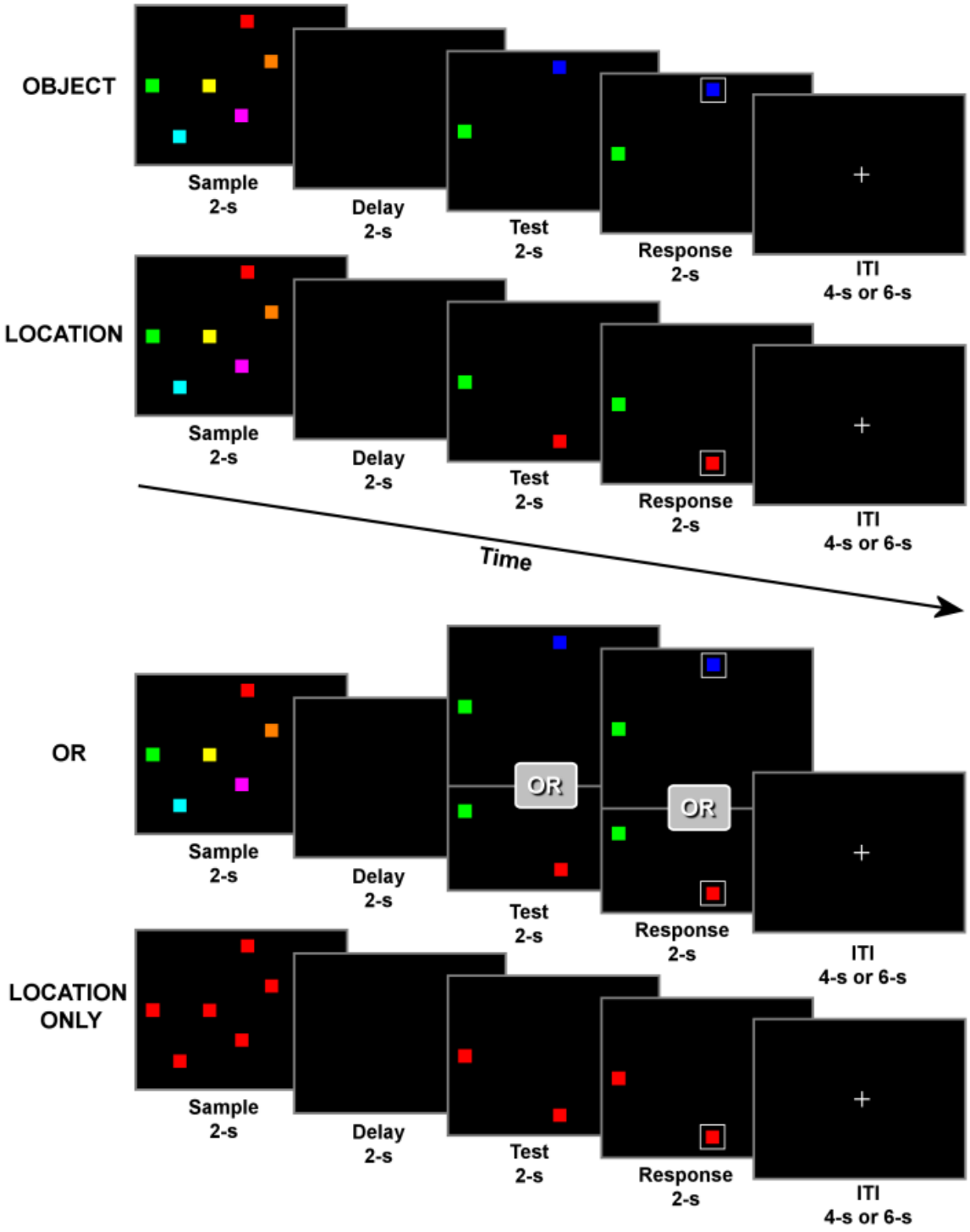

Figure 2.1 Task design and conditions

Schematic of the change detection task for *object* change (first row), *location* change (second row), object *or* location change (third row), and *location only* change which used a single color per trial (fourth row). Each of the four task periods lasted for 2 seconds with a randomly selected inter-trial interval (ITI) of either 4 or 6 seconds.

Behavioral pre-training was conducted up to one week prior to the first fMRI scan to establish familiarity with the task and achieve an acceptable level of performance (> 70%) for each condition. Several fMRI studies have reported significant changes in brain activity corresponding to different stages of training and familiarity for WM tasks (Olesen et al., 2003; Westerberg & Klingberg, 2007), which would likely increase noise across subjects if not properly controlled. A minimum performance criterion of 70% was employed to attenuate this variability. Pre-training consisted of a similar task to the one used in the fMRI for each condition and differed only by the response. During pre-training, subjects made a yes/no response using a computer keyboard rather than a fiber optic button response pad to indicate whether or not the boxed item had changed. Subjects completed 115 trials per condition during the pre-training sessions just as they did during the fMRI session. All subjects were interviewed after each pre-training and imaging session to monitor task strategies.

MRI Acquisition Protocol

Anatomical MRIs were acquired for each of the fifteen subjects. MRI scans were acquired using a 3T Phillips (Bothell, WA) scanner located at the University of Texas Health Science Center at Houston. The scanner was equipped with an eight channel SENSE head coil. High resolution anatomical images were obtained using a magnetization-prepared 180 degree radio-frequency pulse and rapid gradient-echo (MP-RAGE) sequence. Sagittal slices were 1 mm thick and in-plane resolution was 0.938 × 0.938 mm.

fMRI Acquisition Protocol

Functional images were acquired using a gradient recalled echo planar sequence that is sensitive to the blood-oxygen level-dependent (BOLD) signal. With this sequence, 33 axial slices were collected with a 2 s repetition time (TR), a 30ms echo time (TE) and a flip angle of 90˚. Voxel size was 2.75 x 2.75 x 3 mm. Each functional scan series consisted of 153 brain volumes. The first three volumes, collected before equilibrium magnetization was reached, were discarded resulting in 150 usable volumes. Following motion correction and slice timing correction, data were smoothed with a spatial Gaussian filter with a root-mean-square deviation of 3 mm.

fMRI Analysis

fMRI data were analyzed using the Analysis of Functional NeuroImages (AFNI) software (Cox, 1996). While all task periods were processed, only the delay period was used for the primary analyses. Accordingly, functional echo planar image (EPI) data were motion-corrected using a local Pearson's correlation (Saad et al., 2009) and aligned to individual anatomical data for each subject using the 3dAllineate plug-in within AFNI. The data were then normalized for each block by computing percent change from baseline. A deconvolution using a generalized linear model was then computed for each subject using the AFNI function 3dDeconvolve to compute regression coefficients representing activity for a given task period in each voxel for each condition separately. A jitter of the ITI (randomly 4 or 6 s) enabled the deconvolution to properly tease apart

individual trial periods within the hemodynamic response. Within the deconvolution algorithm, an internal test for collinearity was performed for each dataset which passed on the basis of a singular value threshold. Four stimulus regressors corresponding to the four time periods of the task (sample, delay, test, response) were used in the deconvolution analysis. Only trials in which subjects made a correct response were included in the deconvolution analysis. Each regressor was modeled using a boxcar-shaped estimate of the hemodynamic response rather than a temporally-smoothed response function to minimize overlap. To correct for subject motion, six movement regressors were created and included in the deconvolution as regressors of no interest. The resulting coefficients associated with the delay period were transformed to Talairach space using the auto_tlrc algorithm in AFNI.

A similar analysis was performed in order to generate time-series data for each individual subject. This was accomplished by normalizing the data for each block by computing percent change from baseline for each condition and subject. This data was then submitted to a deconvolution algorithm (3dDeconvolve) using a generalized linear model to compute regression coefficients representing activity for a given task period in each voxel for each condition separately. One tent function regressor corresponding to the stimulus of the sample display onset was used in the deconvolution analysis for each condition separately. Only trials for which the subject made a correct response were included in the deconvolution. To correct for subject motion, six movement regressors were also included in the deconvolution as regressors of no interest. The resulting

coefficients were transformed to Talairach space using the auto_tlrc algorithm in AFNI.

fMRI Group Analysis

Individual subject's regression coefficients corresponding to the delay period for correctly-answered trials for each condition were included in a voxel-wise, one-way, repeated measures ANOVA (AFNI program 3dANOVA2). A mixed-effects model was used with subjects (10 for each condition) treated as a random effect factor and conditions (4 total) treated as a fixed-effect factor. The main effects of each fixed factor (condition) were calculated from this ANOVA. *T*-statistics of activation for each condition versus baseline during the delay period were computed at the group-level. Main effects were computed on the basis of an *F* test across the four conditions. In order to correct for multiple comparisons, a spatial cluster extent threshold was applied to the data using a Monte Carlo simulation (1000 randomizations) with an uncorrected voxel-wise threshold of $p < 0.005$. This calculation yielded a threshold of 12 contiguous voxels per cluster. As a result, only activation clusters above that threshold were reported. All results from the ANOVA are projected on the inflated representation of the N27 brain.

2.3 RESULTS

In-Scanner Behavioral Performance

Mean behavioral performance across subjects for the CD task was above 80% for all four conditions (**Figure 2.2**): 83.1% ± 6.7 for the *object condition*, 84.9% ± 7.7 for the *location condition*, 82.1% ± 6.6 for the *or condition*, and 82.1% ± 8.7 for the *location only condition*. There was no significant difference between conditions on the basis of a one-way ANOVA [$F(3,36) = 0.30$, $p = 0.83$]. Mean response times across all four conditions are reported in **Figure 2.3.** Response times were between 800 and 900 ms across all four conditions and were not significantly different [$F(3,36) = 0.32$, $p = 0.80$]. Based on similar behavioral measures, the neural correlates associated with condition differences was known not to correspond to task difficulty across conditions.

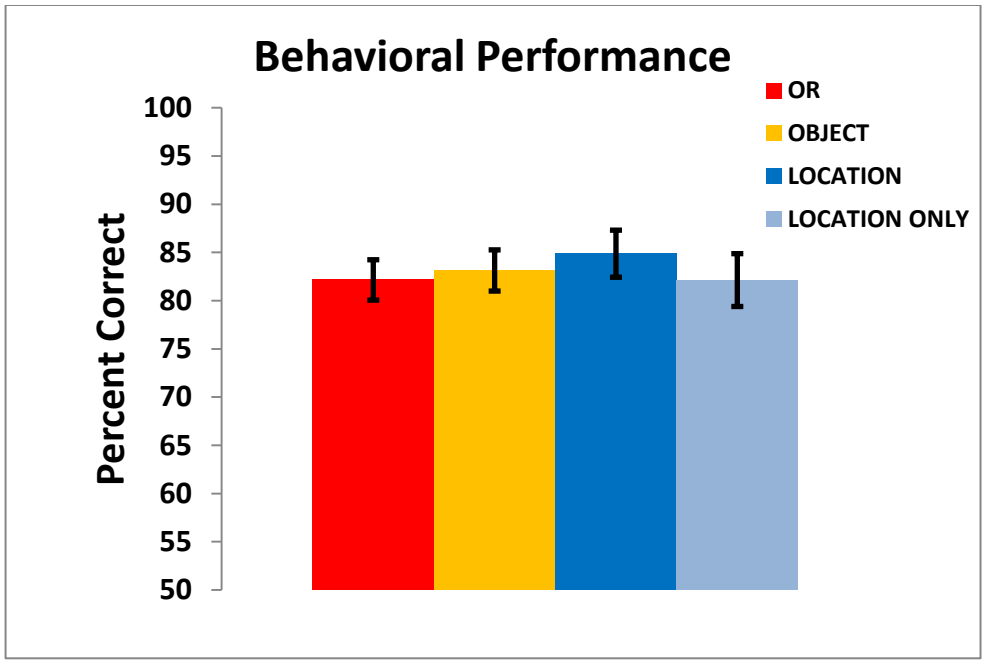

Figure 2.2 fMRI task performance

Behavioral performance in the fMRI scanner for each change detection condition. OR (red), object *or* location change; OBJECT (orange), object change; LOCATION (blue), location change; LOCATION ONLY (light blue), location only change which used a single color per trial.

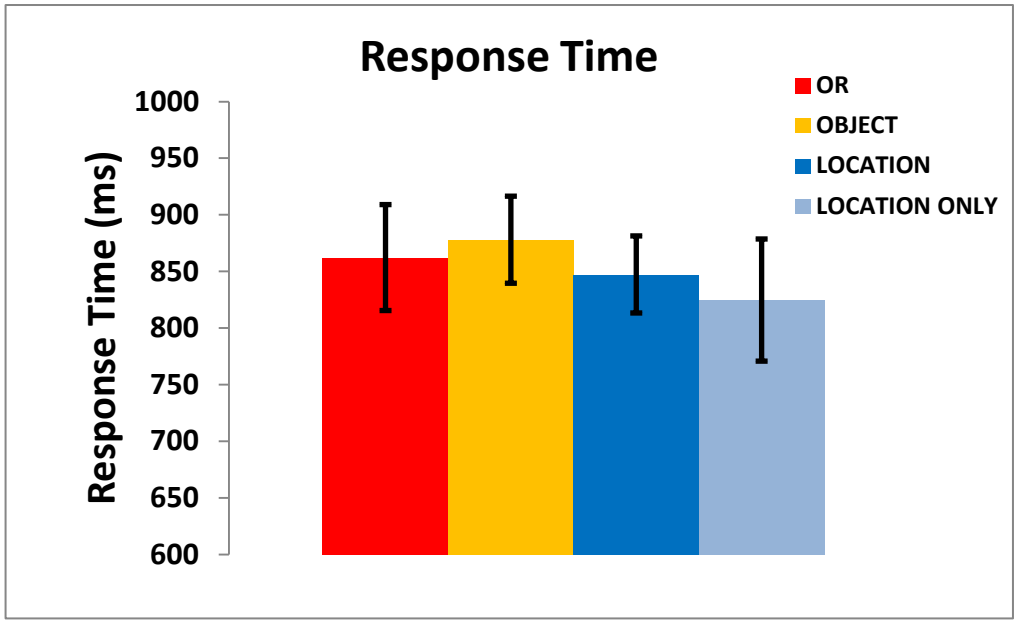

Figure 2.3 fMRI task response time

Response time in the fMRI scanner for each change detection condition. OR (red), object *or* location change; OBJECT (orange), object change; LOCATION (blue), location change; LOCATION ONLY (light blue), location only change which used a single color per trial.

Brain Activation Profiles

The fronto-parietal network described in the fMRI literature (for review see Cabeza and Nyberg, 2000) consists of the DLPFC (portions of Ba 9 & 46) and the IPL and superior parietal lobule (SPL). Accordingly, all four conditions evoked a hemodynamic response in these regions bilaterally (**Figure 2.4**). While parietal activation extended from the SPL more medially to the IPL laterally, activation in the DLPFC was confined to a single posterior region occupying the inferior portion of Ba 9 in the middle frontal gyrus (MFG) in all conditions. The most inferior portion of the DLPFC cluster of activation occupied a superior part of Brodmann area 44 (Ba 44) in the left hemisphere in all but the *location only* condition (**Table 2.1**). Additionally, activation in the pre-supplementary motor area (pre-SMA) was similar across all conditions. Posteriorly, in the occipital lobe, bilateral activation was observed medially in the cuneus and a portion of the lingual gyrus across all conditions. Finally, clusters of activation existed in the middle occipital gyrus bilaterally, also known as the lateral occipital cortex (LOC) (e.g., Malach et al., 1995).

Several clusters of activation were observed to be unique to certain conditions. The insula was activated bilaterally in CD conditions except for the *location only* condition which exhibited no insula activity whatsoever. Conversely, bilateral regions were active in Ba 6 for all conditions except for the *object condition* which exhibited Ba 6 activation in the left hemisphere only. Across conditions, activations were observed in a region within Ba 6, which has been shown to play a role in eye movements and has been termed the frontal eye field

(FEF) (e.g., Fox et al., 1985). Additionally, only the *or* and the *location only* conditions exhibited fusiform activity.

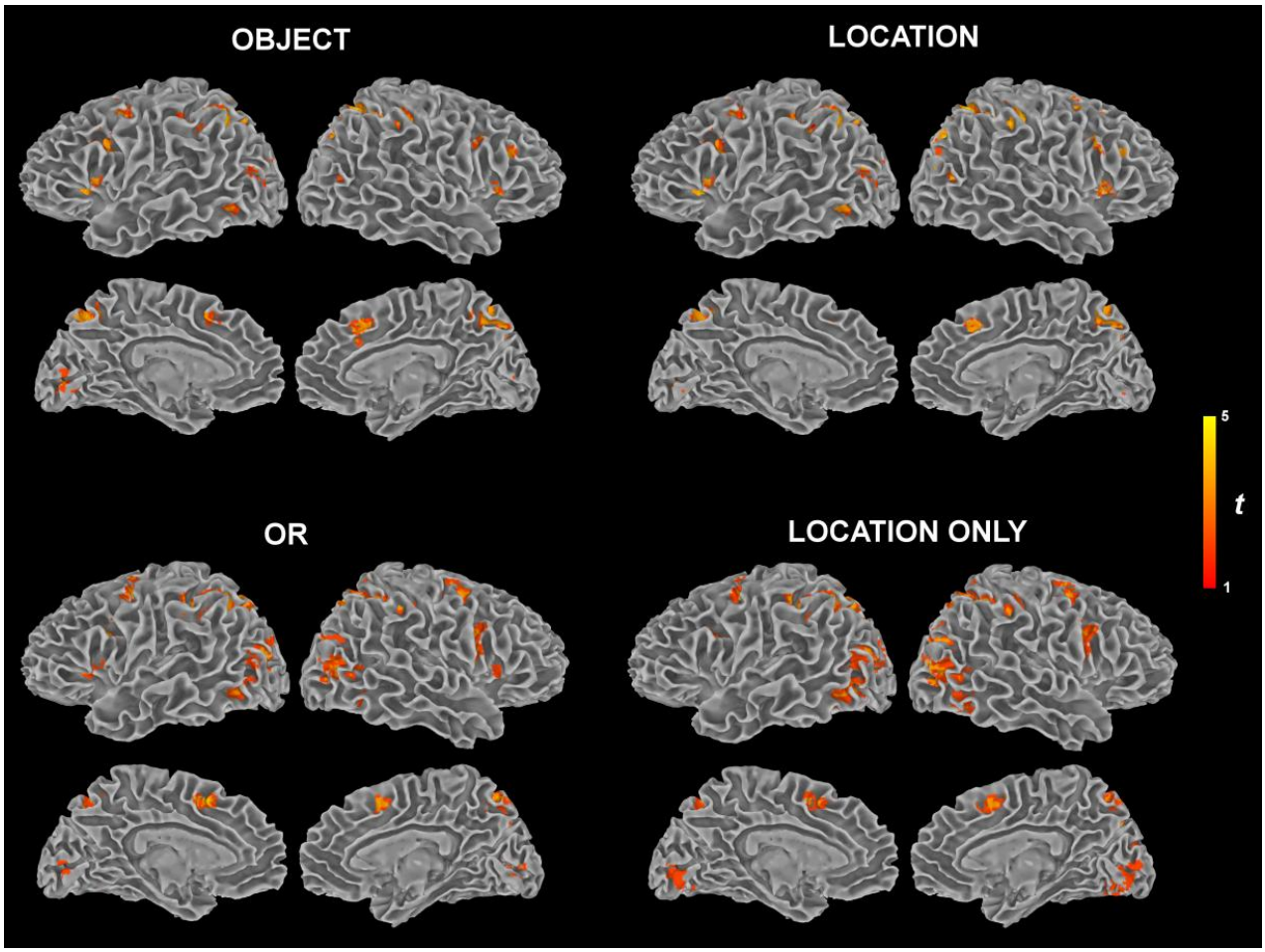

Figure 2.4 Group activation maps for each change detection condition

Statistically significant group activation maps (corrected $p < 0.05$) for each change detection condition. Top left: *object* change, top right: *location* change, bottom left: object *or* location change, bottom right: *location only* change which used a single color per trial.

Condition	Brain Region	BA	Hemisphere	x	y	z	*t*-value
Object	superior parietal lobule, inferior parietal lobule, cuneus, precuneus	40	L	27.0	57.0	44.0	4.924
	superior parietal lobule, inferior parietal lobule, precuneus	40	R	-29.0	63.0	42.0	4.413
	inferior frontal gyrus, middle frontal gyrus	9	L	37.0	-7.0	26.0	3.776
	medial frontal gyrus, cingulate	8	L+R	-3.0	-21.0	38.0	3.653
	cuneus, precuneus	19	R	-25.0	81.0	30.0	3.430
	middle frontal gyrus, superior frontal gyrus	6	L	35.0	1.0	48.0	3.572
	lingual gyrus	18	L	3.0	79.0	4.0	3.403
	insula	13	L	27.0	-21.0	4.0	3.902
	middle frontal gyrus	9	R	-49.0	-7.0	32.0	3.280
	middle frontal gyrus	46	R	-47.0	-23.0	24.0	3.568
	middle occipital gyrus	19	R	-39.0	67.0	10.0	3.261
	insula	13	R	-33.0	-21.0	0.0	3.456
	middle occipital gyrus	37	L	41.0	61.0	-6.0	3.230
Location	superior parietal lobule, inferior parietal lobule, cuneus, precuneus	40	L	27.0	57.0	46.0	4.536
	superior parietal lobule, inferior parietal lobule, precuneus	40	R	-47.0	33.0	42.0	4.195
	cuneus, precuneus	19	R	-29.0	73.0	34.0	3.569
	middle frontal gyrus	9	L	33.0	-15.0	24.0	3.614
	insula	13	L	27.0	-21.0	4.0	3.786
	middle frontal gyrus, superior frontal gyrus	6	L	35.0	3.0	48.0	3.350
	insula	13	R	-33.0	-19.0	4.0	3.340
	medial frontal gyrus, cingulate	8	L+R	-7.0	-21.0	38.0	3.318
	lingual gyrus	18	L	7.0	79.0	0.0	3.029
	middle frontal gyrus	9	R	-49.0	-10.0	34.0	3.257
	middle frontal gyrus	46	R	-47.0	-23.0	24.0	3.392
	middle occipital gyrus	37	L	41.0	61.0	-6.0	3.200
	middle frontal gyrus, superior frontal gyrus	6	R	-29.0	-1.0	52.0	3.084
Or	superior parietal lobule, inferior parietal lobule, cuneus, precuneus, middle occipital gyrus	40	R	-29.0	47.0	38.0	4.597
	superior parietal lobule, inferior parietal lobule, cuneus, precuneus, middle occipital gyrus	40	L	33.0	49.0	40.0	4.409
	middle frontal gyrus, superior frontal gyrus	6	L	31.0	3.0	48.0	3.779
	middle frontal gyrus, superior frontal gyrus	6	R	-33.0	3.0	50.0	4.334
	inferior frontal gyrus, middle frontal gyrus	9	R	-49.0	-3.0	30.0	3.713
	medial frontal gyrus, cingulate	6	L+R	3.0	-9.0	46.0	4.180
	lingual gyrus	18	L	-3.0	83.0	2.0	3.049
	fusiform gyrus	37	R	-47.0	55.0	-12.0	3.208
	insula	13	L	27.0	-21.0	4.0	3.280
	insula	13	R	-33.0	-21.0	6.0	3.063
	lingual gyrus	18	R	-13.0	73.0	4.0	2.916
Location Only	superior parietal lobule, inferior parietal lobule, cuneus, precuneus, middle occipital gyrus, fusiform gyrus, lingual gyrus	40	R	-45.0	35.0	40.0	4.574
	superior parietal lobule, inferior parietal lobule, cuneus, precuneus, middle occipital gyrus, fusiform gyrus, lingual gyrus	40	L	27/0	75.0	22.0	4.745
	middle frontal gyrus, superior frontal gyrus	6	L	27.0	5.0	46.0	3.828
	middle frontal gyrus, superior frontal gyrus	6	R	-29.0	3.0	50.0	4.074
	middle frontal gyrus	9	R	-47.0	-3.0	28.0	3.936
	medial frontal gyrus, cingulate	32	L+R	-7.0	-11.0	44.0	3.782
	inferior frontal gyrus, middle frontal gyrus	9	L	41.0	-5.0	24.0	3.750

Table 2.1 Cluster analysis for each change detection condition

Clusters of activation are significant at a corrected $p < 0.05$ for each change detection condition. L= left hemisphere, R = right hemisphere, L+R = a single cluster extending from one hemisphere to the other. Talairach coordinates correspond to peak activation within a cluster.

The main effects of neural activity from the four conditions are illustrated in **Figure 2.5**. The data analysis yielded six loci including the left DLPFC, the right IPL, the LOC bilaterally, and the fusiform gyrus (FUS) bilaterally (**Table 2.2**). Time-courses associated with each of the six clusters of activation were generated for each condition (**Figure 2.5a – f**) with activation for each 2 second period over a 14 second window. Accordingly, clusters appear to correspond to location or object identity memory conditions. The onset of the first stimulus for each trial, the sample period, corresponds to the 0 second time point. The lag associated with peak hemodynamic response has been shown to be 4 to 6 seconds post-stimulus (Bandettini et al., 1992) which suggests that the 8 second time-point likely corresponds to delay period activity. Activity for the *object* (seen in orange) and *or* (seen in red) conditions, both of which require the subjects to remember the identities of each item, is greater in the left DLPFC cluster when compared to the *location* (seen in blue) and *location only* (seen in light blue) conditions (**Figure 2.5a**). A similar grouping of conditions along with greater activity associated with object-related conditions was found in the left fusfiform gyrus (**Figure 2.5e**).

Posterior clusters (e.g., LOC and IPL) exhibit greater activation for location memory conditions. Specifically, bilateral LOC clusters (**Figure 2.5c** & **Figure 2.5d**) exhibit a gradient of activation such that the *location* activity was greater, followed by the *location only* and *or* conditions, and finally the *object* condition which appears to be at or below baseline activity at the 8 s time-point. The cluster in IPL shows a similar degradation across conditions, with the *location*

only condition exhibiting greater activity than the *or condition* (**Figure 2.5b**). The right fusiform cluster appears to correspond to the *location only* condition while all other conditions exhibit significantly weaker activations. As the *location* and the *object* conditions demonstrate similar activations, this region cannot be purely associated with location memory.

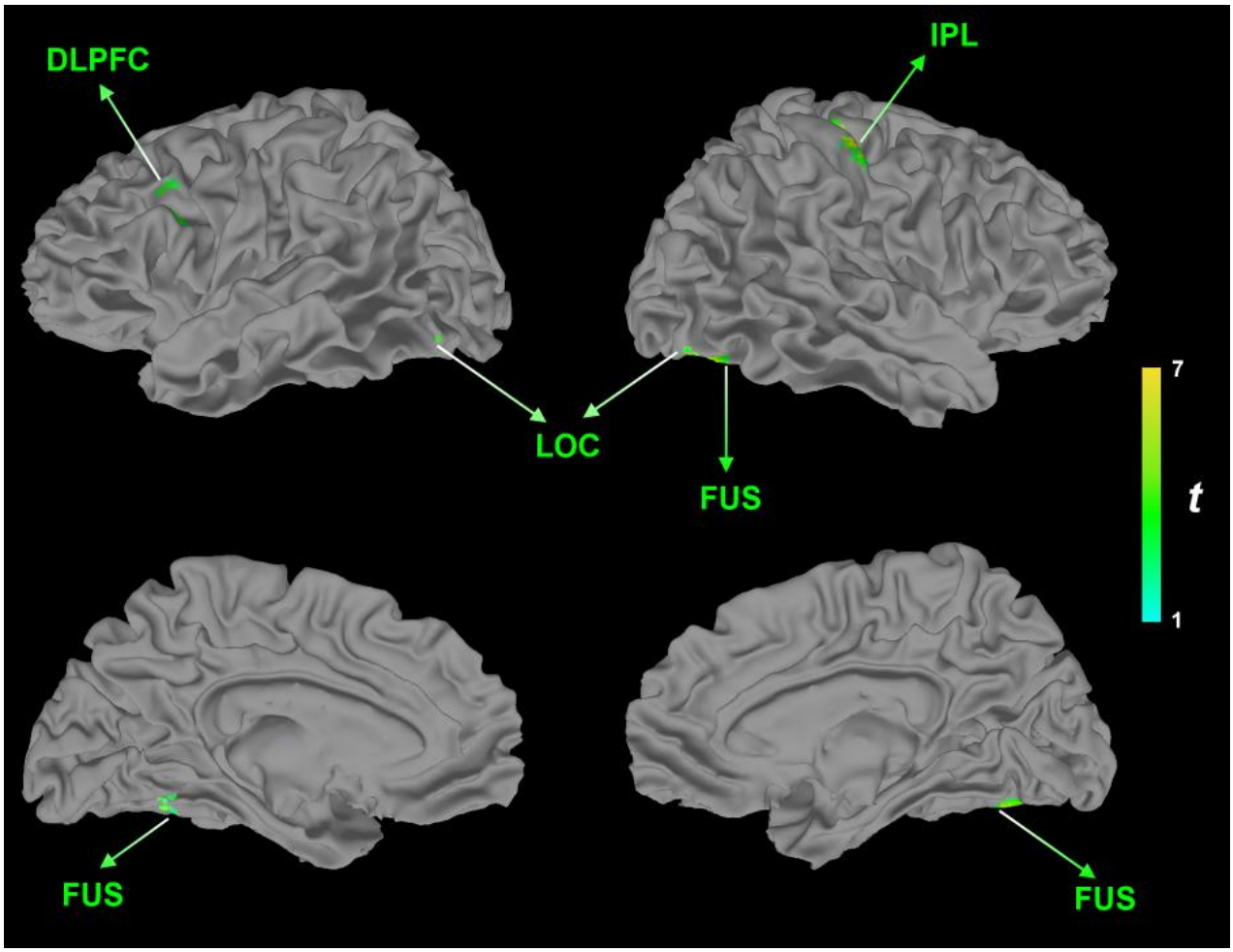

Figure 2.5 Main effect of fMRI task condition

Group activation map of the main effect of neural activity across change detection conditions. Activations are significant at a corrected $p < 0.05$. Labeled regions: DLPFC, dorsolateral prefrontal cortex; IPL, inferior parietal lobule; FUS, fusiform gyrus; LOC, lateral occipital cortex.

Brain Region	BA	Hemisphere	x	y	z	*t*-value
inferior parietal lobule, postcentral gyrus	40	R	-37.0	27.0	54.0	4.133
fusiform gyrus	19	L	-35.0	65.0	-18.0	4.196
middle occipital gyrus, inferior temporal gyrus	19	L	53.0	64.0	0.0	4.510
middle occipital gyrus, inferior temporal gyrus	19	R	-48.0	-69.0	1.0	3.912
middle frontal gyrus	9	L	43.0	-7.0	30.0	4.014
fusiform gyrus	19	R	29.0	58.0	11.0	3.749

Table 2.2 Cluster analysis of condition effect

Clusters of activation represent condition effect across change detection conditions and are significant at a corrected $p < 0.05$. L= left hemisphere, R = right hemisphere, L+R = a single cluster extending from one hemisphere to the other. Talairach coordinates correspond to peak activation within a cluster.

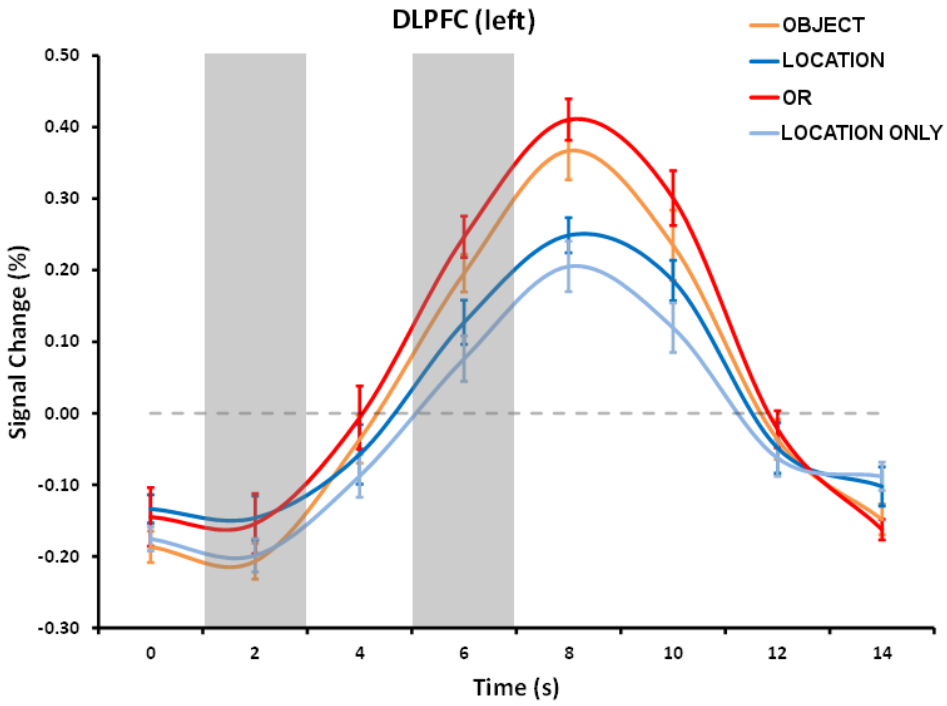

Figure 2.5a Left DLPFC time-course

Trial-averaged time-courses of the estimated response within the left DLPFC activation from Figure 2.5. Error bars represent standard errors of the mean. Gray bars indicate sample and test periods respectively.

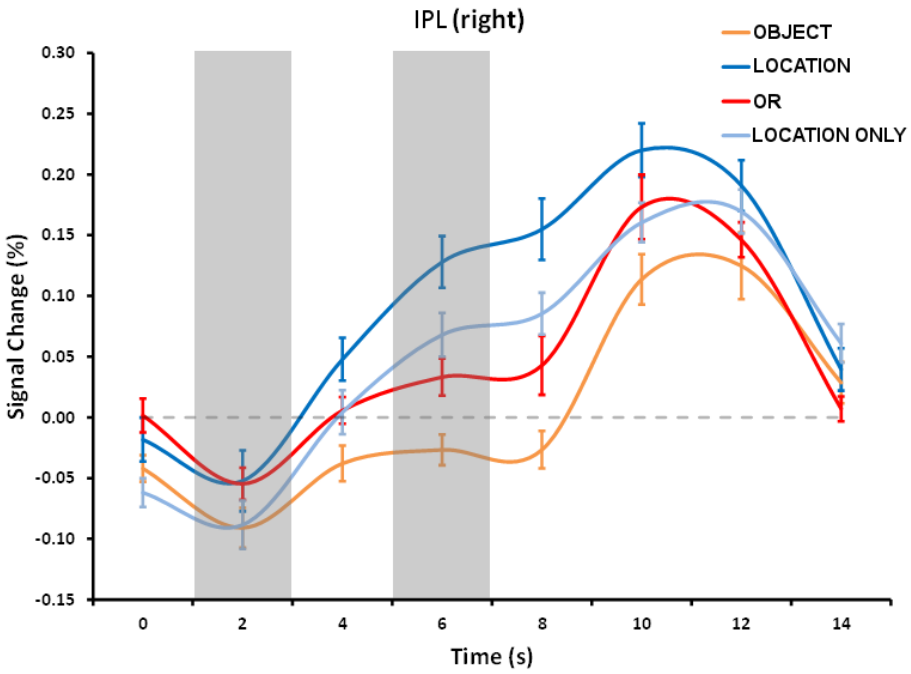

Figure 2.5b Right IPL time-course

Trial-averaged time-courses of the estimated response within the right IPL activation from Figure 2.5. Error bars represent standard errors of the mean. Gray bars indicate sample and test periods respectively.

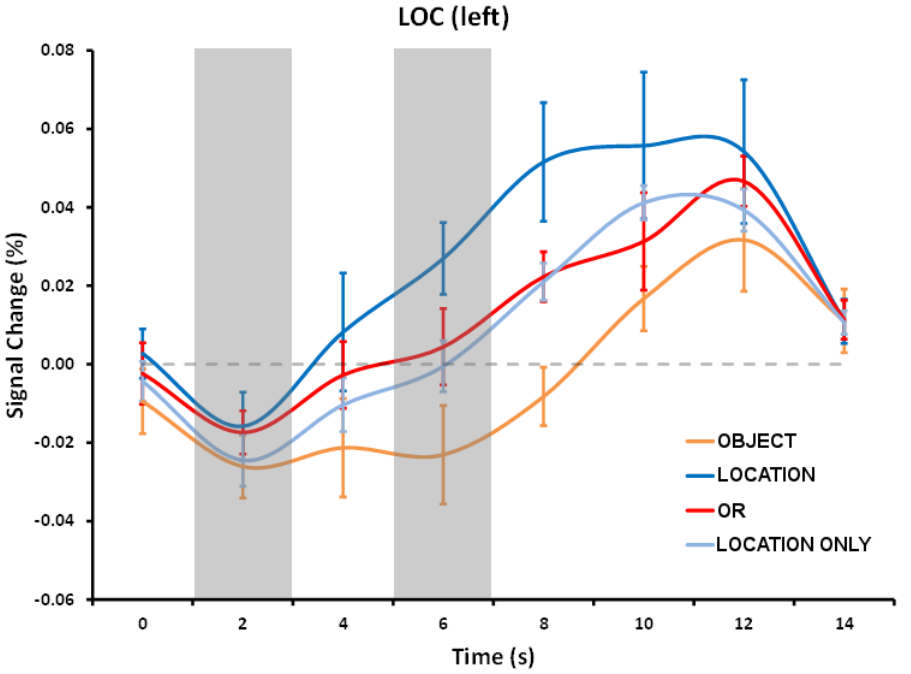

Figure 2.5c Left LOC time-course

Trial-averaged time-courses of the estimated response within the left LOC activation from Figure 2.5. Error bars represent standard errors of the mean. Gray bars indicate sample and test periods respectively.

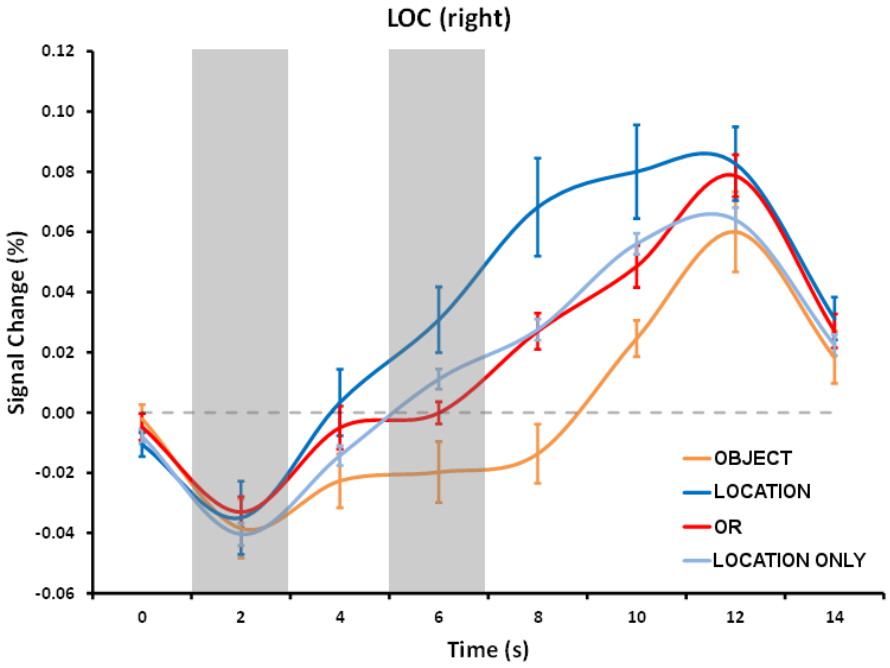

Figure 2.5d Right LOC time-course

Trial-averaged time-courses of the estimated response within the right LOC activation from Figure 2.5. Error bars represent standard errors of the mean. Gray bars indicate sample and test periods respectively.

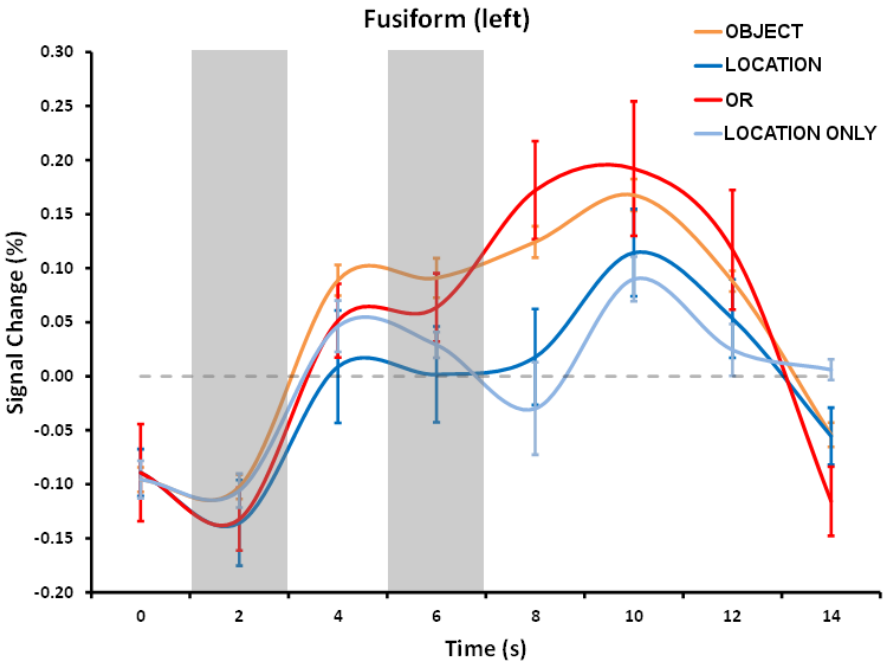

Figure 2.5e Left fusiform time-course

Trial-averaged time-courses of the estimated response within the left fusiform activation from Figure 2.5. Error bars represent standard errors of the mean. Gray bars indicate sample and test periods respectively.

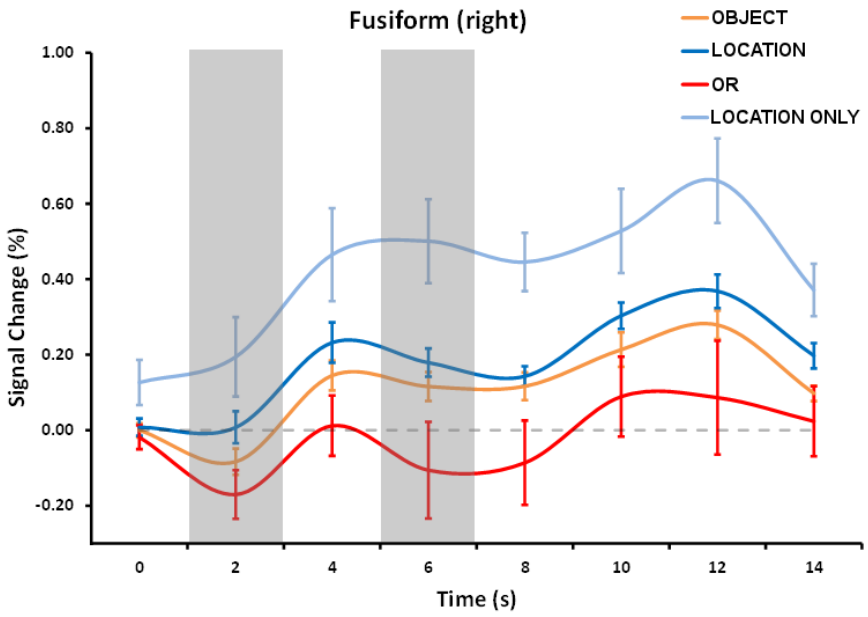

Figure 2.5f Right fusiform time-course

Trial-averaged time-courses of the estimated response within the right fusiform activation from Figure 2.5. Error bars represent standard errors of the mean. Gray bars indicate sample and test periods respectively.

2.4 DISCUSSION

The aims of this experiment were: (1) identify a dissociation corresponding to location and object identity VWM, and (2) determine if the results corresponded to a caudal-rostral in contrast to a dorsal-ventral interpretation of VWM dissociation. Accordingly, we identified a main effect resulting from a direct comparison of VWM conditions. Although all conditions shared a common profile of activation, there were subtle differences in specific regions suggesting a caudal-rostral interpretation of location and object identity memory.

Generally, blood-oxygen-level dependent (BOLD) activation profiles associated with the brief delay period in each of the four conditions reported here

are in agreement with the literature on VWM (e.g., Mohr et al., 2006; Sala & Courtney, 2007). Short delays allow for a more direct comparison across other imaging techniques such as MEG and electroencephalography (EEG) which typically require many more trials (n > 100) than fMRI in order to achieve a clear neural representation of activity. The use of a longer delay (more than 9 s for example) would preclude the study of this task using MEG or EEG due to the extremely long scanning duration required. Accordingly, our results suggest that it is possible to image the delay period of a VWM task with a relatively short delay of 2 s which provide concordant VWM results with those reporting both short (1.5 s) and long delays (9 s) (Todd & Marois, 2004; Todd et al., 2011).

During the delay period, the subject worked to maintain the sample information in mind which is supported by activity in the DLPFC and parietal lobe structures (e.g., Damoiseaux et al., 2006; Seeley et al., 2007). Furthermore, studies have reported this fronto-parietal network to be active only during the maintenance and manipulation of information (e.g., Miller & Cohen, 2001; Muller & Knight, 2006; Petrides 2005). We found delay period activity localized to a more posterior and dorsal region occupying BA 9 in all conditions and extended anteriorly to BA 46 of the DLPFC in the *object* and *or* conditions. This shift across conditions may correspond to divergent functional roles of DLPFC sub-regions, a structure which has been characterized generally as the center for goal-directed behavior (Miller & Cohen, 2001; Stuss & Levine, 2002). Concerning parietal structures, we showed activity in both the left and right IPL, which has been

shown to correspond to memory maintenance and positively correlate with memory load (e.g., Todd & Marois, 2004).

While the pre-SMA region was activated in all CD conditions, no effect of condition was observed across conditions likely suggesting a role in executive function common to WM in general. An early study by Petit et al. (1998) demarcated the medial motor areas active during various working memory and motor tasks to disambiguate the role of the pre-SMA region during working memory tasks. They concluded that activation in the pre-SMA region during delay periods reflects a state of "preparedness" for selecting a motor response on the basis of maintained information. Since all four VWM conditions in this experiment required a motor response (button press) at the end of every trial, similar pre-SMA activity across conditions was observed.

Dissociation of Location and Object Identity VWM Using fMRI

In accordance with the first aim of this experiment, a main effect of condition resulting from a direct comparison of CD conditions yielded a dissociation of location and object identity VWM. Specifically, activation in the right mid-fusiform gyrus coincided with greater activity for the *location only* condition compared to all other CD conditions. The fusiform gyrus has classically been described as the functional source of face and complex item recognition (e.g., Clark et al., 1996; Puce et al., 1995). The right fusiform face area (FFA) has been implicated in the configural processing of faces (e.g., Rossion et al., 2000). Less is known about the sub-regions within the fusiform gyrus which

neighbor the FFA including the mid-fusiform region. Recently, it has been suggested that the left mid-fusiform gyrus plays a role in language processing (e.g. Glezer et al., 2009; Ma et al., 2011). Conversely, the right mid-fusiform region has been implicated in configural object processing (e.g., Hocking & Price, 2009; Shen et al., 1999). The *location only* condition required configural processing with regards to the global configuration of the 6-item display. While the *location* and *or* conditions required similar processing, the uniform color among items presented in the *location only* condition provided a more unified and holistic configuration as compared to all other conditions.

Only a few fMRI studies on VWM have identified the insula as an active region during the delay period (e.g., Borowsky et al., 2005; Sala et al., 2003; Todd et al., 2011), while Ba 6 (i.e., the FEF region), has been implicated in various fMRI studies across a broad range of working memory tasks (for review see Cabeza & Nyberg, 2000). The LOC has been defined as extending from the lateral portion of the middle occipital gyrus to the posterior inferior temporal gyrus bilaterally and it has been suggested that the LOC is the primary locus of object identity representation (Grill-Spector, 2003; Malach et al., 1995; Op de Beeck et al., 2008). However, recent fMRI studies have posited that the LOC may play a substantial role in processing spatial information as well (Cichy et al., 2011; Kravitz et al., 2008). Accordingly, our finding of activation in the LOC across both location and object identity WM conditions is in agreement with these recent reports suggesting a split role within the LOC.

Previous fMRI studies have identified the left DLPFC as an important region for processing object-related memory (for review see Levy & Goldman-Rakic, 2000). For example, a recent study by Sala and Courtney (2007) studied VWM using an object memory condition, a location memory condition, and a combined object and location memory condition. Findings from this study suggested an object greater-than location separation within the left DLPFC (IFG and MFG). Moreover, the activation of the condition requiring the memory of both object and location information was similar to activation associated with the object condition, both of which were greater than the location condition. Our findings confirm those reported in the study by Sala and Courtney based on the time-course plot in **Figure 2.5a**. A similar dissociation has been recently reported in several fMRI experiments studying object and location WM (Leung & Alain, 2011; Mohr et al., 2006; Sala et al., 2003). Additionally, early reviews of the WM literature studying object and location memory demonstrate a preponderance of object memory findings in the left DLPFC (Cabeza & Nyberg, 2000; Courtney et al., 1998; Levy and Goldman-Rakic, 2000; Owen, 2000).

The finding of greater location than object memory in a right parietal region (IPL) has been reported in previous studies of WM using fMRI (e.g., Leung & Alain, 2011; Sala & Courtney, 2007). A recent fMRI study by Harrison et al. (2010) used an inferior parietal sulcus (IPS) localizer across subjects and measured differences associated with increased object and location workload within that region. The IPS in both hemispheres demonstrated an increase in activity associated with increased location workload but not an increase in object

workload. The authors conclude that capacity-related activation observed in the IPS is mainly driven by spatial representations. Our results (**Figure 2.5b**) are in agreement with this finding within the right hemisphere. Specifically, a region neighboring the IPS which occupies Ba 40 and an anterior portion of the IPL demonstrated greater activation for location memory conditions when compared to conditions recruiting the use of object identity memory. Previous meta-analyses have also implicated the right IPL (along with neighboring parietal structures) as a brain region responsible for location memory (Cabeza & Nyberg, 2000; Courtney et al., 1998; Wager & Smith, 2003).

A Caudal-Rostral Interpretation Using fMRI

Several fMRI experiments studying WM have focused their analysis on dorsal and ventral prefrontal regions in an attempt to identify a location-object dissociation, respectively, with varying results (Mohr et al., 2006; Rama et al., 2004; Sala et al., 2003; Sala & Courtney, 2007; Volle et al., 2008). Upon closer inspection, these studies reveal a dissociation within a caudal-rostral interpretation of location and object identity VWM. The experiment by Sala et al. (2003) reports a preponderance of neural activity associated with location conditions in occipital and parietal structures with activation extending into Ba 6 in the frontal lobe. In contrast, the identity conditions appear to be limited to anterior temporal regions and prefrontal regions including Ba 9 and 46 bilaterally. Similarly, four recent fMRI studies show the same dissociation across studies whereby spatial memory activity is localized to superior parietal structures and superior Ba 6 while object memory is localized to left anterior prefrontal

structures including the inferior frontal gyrus (IFG) and the MFG (Rama et al., 2004; Mohr et al., 2006; Volle et al., 2008; Sala & Courtney, 2007). Two early imaging studies by Haxby et al. (1994) and Courtney et al. (1996) published a decade earlier than the aforementioned studies indirectly suggest a similar caudal-rostral dissociation extending from posterior parietal regions and superior Ba 6 for location memory to more anterior prefrontal regions in the DLPFC. Therefore, our findings of a location-object separation within a caudal-rostral framework appear to be indirectly in agreement with previous studies which do not explicitly mention such a framework although it is apparent from their findings. Specifically, results from our experiment suggest that caudal structures (LOC and IPL) demonstrate greater activity for location memory conditions while a rostral area (left DLPFC) shows greater activity for object identity memory. Based on the main effect of task conditions, no dorsal-ventral separation corresponding to location and object memory was found. This finding addresses the second aim of this experiment and suggests that a caudal-rostral interpretation as compared to a dorsal-ventral interpretation more accurately reflects dissociations of location and object identity memory.

CHAPTER 3

SEPARATING OBJECT AND LOCATION WORKING MEMORY USING MEG

3.1 INTRODUCTION

One of the main aims of this study was to provide convergent evidence across two different imaging methods (fMRI and MEG) within the context of location and object identity VWM. These two methods are complimentary in that fMRI provides high spatial resolution at the millimeter level while MEG provides high temporal resolution, capable of detecting signals at the sub-millisecond level. Accordingly, neural oscillations are detectable using MEG, which may be broken down into time and frequency ranges on the basis of a Fourier transform of the recorded flux data. Amplitudes associated with each frequency range are approximated for small time windows to determine if a signal (e.g., an MEG channel) is phase-locked to the timing of a stimulus. Increases in neural oscillations within a frequency range relative to baseline activity (typically pre-stimulus periods) are considered event-related synchronizations (ERS) while decreases are considered event-related desynchronizations (ERD). Both components have been shown to play a role in VWM depending on the frequency band observed (e.g., Grimault et al., 2009; Robitaille et al., 2009). While recent intracranial EEG studies have implicated very fast oscillations (gamma and high gamma frequencies, greater than 100 Hz) in VWM processes (e.g., Khursheed et al., 2011; Meltzer et al., 2008), it is unlikely that such fast signals are detectable by MEG due to the weak amplitude associated with this frequency range (e.g., Meltzer et al., 2008). Therefore, slower frequency ranges including beta (13-30 Hz), alpha (8-13 Hz), and theta (4-8 Hz) are studied in the

MEG/EEG literature focusing on VWM (e.g., Düzel et al., 2003; Palva et. al., 2010; Raghavachari et al., 2001).

While data analysis techniques for describing the hemodynamic response in fMRI experiments have been fairly consistent across studies, the analysis of MEG data is less so. The primary challenge is associated with the source analysis of MEG data, which requires localizing electric activity within the brain on the basis of induced magnetic fields detected outside of the brain. This problem is termed the *inverse problem*, which has no unique solution. Therefore, the driving force behind developing new MEG analysis techniques is exploring the "best" solution among all possibilities. Earlier MEG studies used an equivalent current dipole (ECD) approach to localize event-related fields (ERFs) (e.g., Sarvas, 1987; Simos et al., 2000) and helped establish this technique as the clinical gold standard for basic motor and language mapping (e.g., Papanicolaou et al.,1999). Recently, the MEG field has seen a shift to more dynamic approaches in an attempt to address the inverse problem, namely distributed source approaches, which employ localization algorithms to determine the most likely source distribution among many possibilities. MEG studies focusing on VWM have used both the ECD approach (e.g., Campo et al., 2004; Pazo-Alvarez et al., 2008) and the distributed source approach (e.g., Robitaille et al., 2009; Palva et al., 2011) in the form of a spatially adaptive filter termed a beamformer.

Among the VWM neuroimaging literature, only one MEG study (Jokisch & Jensen, 2007) has focused on directly comparing memory for object identities

and locations. Although it could be argued that spatial orientations are also object identities, the investigators of the MEG study were able to compute different neural activations associated with each object and location condition. Posterior activity within the dorsal stream, near the parieto-occipital sulcus, was shown to be inhibited during the object identity condition in favor of a visual dorsal-ventral model. No additional MEG studies have explicitly studied object and location VWM in an effort to tease apart memories associated with either domain.

In order to study a behavior across multiple imaging techniques it is important to understand the relationship between recorded neural magnetic (MEG) and electric (EEG) fields and the BOLD response of fMRI. Recent evidence establishing a relationship between fMRI and MEG/EEG imaging modalities has done so in the context of specific frequency ranges of MEG/EEG data (e.g., Khursheed et al., 2011). Specifically, increases in gamma range activity has been shown to positively correlate with increases in the observed BOLD response across similar regions (Gaetz et al., 2011; Khursheed et al., 2011; Logothetis, 2002; Meltzer et al., 2008). Concerning beta and alpha band activity, both positive (e.g., Gonçalves et al., 2006; Mitsuru et al., 2010; Stevenson et al., 2011) and negative (e.g., Callan et al., 2010; Zumer et al., 2010) correlations associated with increased BOLD activity have been reported. Concerning theta band activity, various studies have shown both positive and negative correlations with the observed BOLD response (e.g., Scheeringa et al., 2009; Michels et al., 2010).

Utilizing four change detection conditions testing for location and object identity VWM, the MEG findings corresponding to each condition and their activations are reported here. According to the results we obtained from fMRI, we hypothesize that theta oscillations will localize to fronto-parietal and occipital regions demonstrating a caudal-rostral interpretation of location and object identity memory across conditions in this experiment.

3.2 MATERIALS & METHODS

Subjects

Fourteen healthy subjects (six men, 23-33 years old) participated in the MEG experiment and provided written informed consent and were compensated financially for their time. Among these fourteen subjects, twelve participated in the fMRI study. A total of ten subjects participated in each of the four task conditions. Study procedures were approved by the University of Texas Health Science Center at Houston Institutional Review Board. All subjects were in good health with no history of psychiatric or neurological disease and had normal or corrected-to-normal (with contact lenses) visual acuity.

Task

The stimulus and task parameters across all four conditions are outlined in detail in **2.2** for the fMRI experiment. Identical tasks including stimulus displays and timing parameters were used for the MEG experiment. Subjects were tested in 4 memory conditions for both experiments: change detection for object

identities requiring the subject to remember the color of each square (*object condition*), change detection for locations (*location condition*), change detection for objects and locations with the subject unaware as to which property of the square would change (*or condition*), and change detection for locations with uniform color across trials (*location-only condition*) (**Figure 2.1**). Stimuli for MEG scans were reflected from a projector onto a screen in front of the subject with a viewing angle of 30.0 degrees. Due to differences in viewing angle across fMRI and MEG methods, the stimuli were resized for MEG scans to produce identical viewing angles for each stimulus.

Behavioral pre-training was conducted up to one week prior to the first MEG or fMRI scan to establish familiarity with the task and achieve an acceptable level of performance (at least 70%) for each condition. Pre-training consisted of a similar task to the one used in the MEG for each condition and differed only by the response. During pre-training, subjects made a yes/no response using a computer keyboard rather than a fiber optic button response pad to indicate whether or not the boxed item had changed. Subjects completed 115 trials per condition during the pre-training sessions, identical to the number of trials for the MEG session. All subjects were interviewed after each pre-training and imaging session to monitor task strategies.

MRI Acquisition Protocol

Structural MRIs were acquired for each subject to be later used for MEG source localization. MRI scans were acquired using a 3T Phillips (Bothell, WA)

scanner located at the University of Texas Health Science Center at Houston. The scanner was equipped with an eight channel SENSE head coil. High resolution anatomical images were obtained using a magnetization-prepared 180 degree radio-frequency pulse and rapid gradient-echo (MP-RAGE) sequence. Sagittal slices were 1 mm thick and in-plane resolution was 0.938 × 0.938 mm.

MEG Acquisition Protocol

MEG signals were recorded using a whole-head MEG system with 248 axial gradiometers (WH 3600, 4D Neuroimaging, San Diego, California, USA). Signals were digitized at a sampling rate of 508.63 Hz and filtered online with a 0.1 Hz high-pass filter. Data were noise-reduced offline using separate reference gradiometers to record environmental noise and algorithm from the 4D-Neuroimaging software. head position information was acquired before and after each MEG acquisition.

MEG Analysis

All MEG data were processed using the FieldTrip toolbox developed at the F.C. Donders Centre for Cognitive Neuroimaging (http://www.ru.nl/fcdonders/fieldtrip/). While all MEG data were processed, only the delay period was included in the primary data analyses. Each condition for each subject was separated from condition-paired MEG sessions and analyzed individually. Within each condition, trials which were contaminated by artifacts such as eye movement or other motor movements were removed from the data. Furthermore, an independent component analyses (ICA) algorithm was used to

classify and remove cardiac artifacts and additional artifact components related to eye movements. The resulting artifact-free signals for each condition were used for all further analyses procedures. A time-frequency (TF) analysis was performed by applying a Morlet wavelet-based transform to the single-trial time-series with a window length of 1 and a step size of 0.5. Each TF period was normalized to the pre-stimulus activity (baseline) before being averaged across trials. Plots were constructed with a frequency range of 3 to 95 Hz and a period of 0 to 9 seconds (-500 to 0 ms baseline) with all trials averaged across individual conditions for each subject and then averaged across subjects (**Figure 3.1**). No significant ERS or ERD were observed in the gamma range (30-95 Hz). However, lower frequency ranges (< 30Hz) exhibited significant changes in oscillatory power with respect to baseline activity. Accordingly, **Figure 3.2** illustrates the same TF plots with a reduced frequency range (3 to 30 Hz). Furthermore, clusters of spectra data which are significantly greater (ERS) or less than (ERD) baseline amplitude are outlined in white for each condition. In order to compare the post-stimulus spectra to the pre-stimulus (baseline) spectra, the data was reduced in both frequency and latency to decrease the resolution of the spectra and provide fewer comparisons when performing a dependent samples t-test for each spectra point. A distribution of cluster-level *t* statistics was computed from a Monte Carlo simulation of 1000 randomizations and only spectra clusters meeting statistical significance (corrected $p < 0.05$) are outlined in white (**Figure 3.2**).

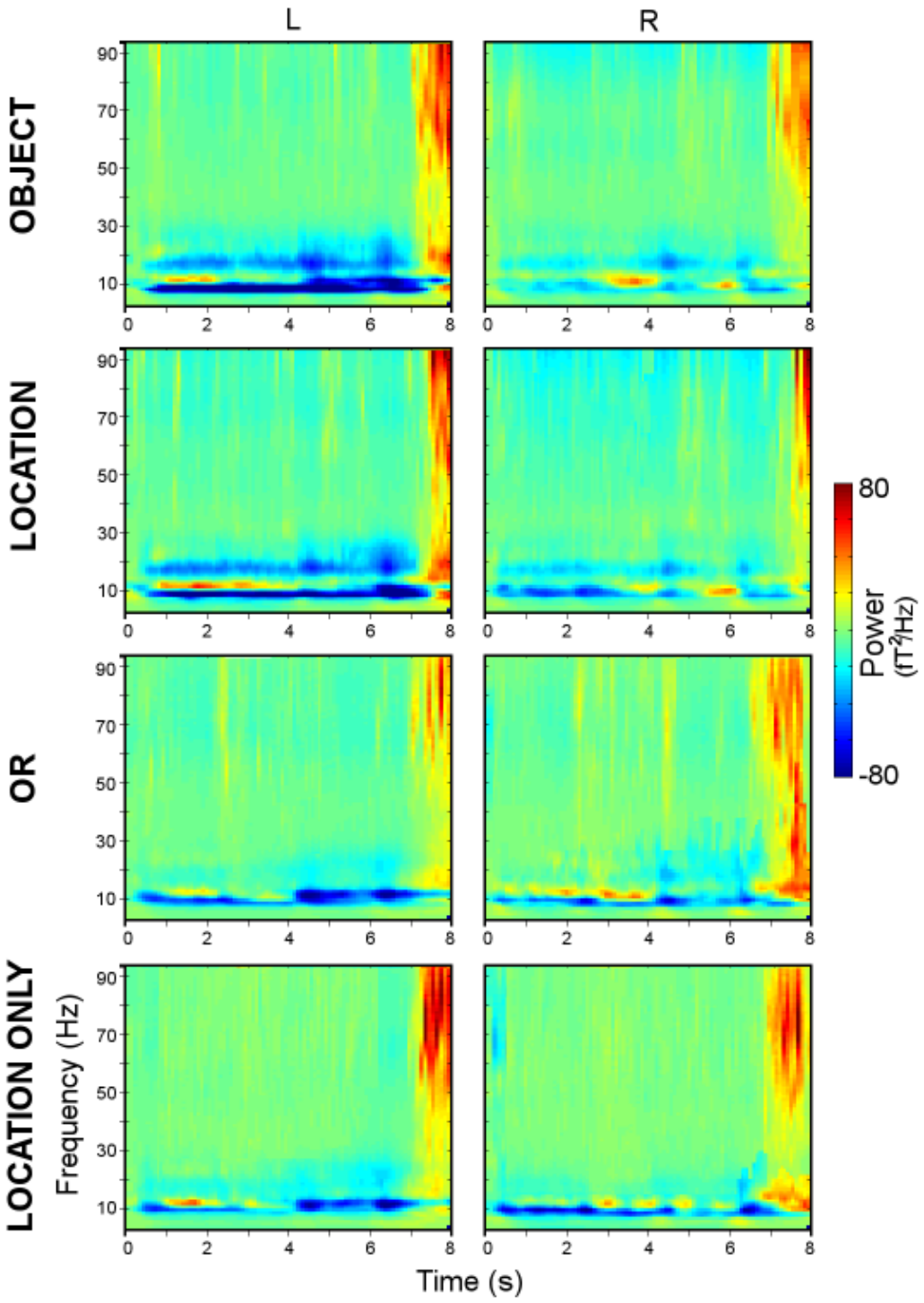

Figure 3.1 Time frequency plots (3 to 95 Hz)

Time-frequency plots from left and right MEG sensors covering the left and right lateral temporal regions, respectively, with a frequency range of 3 to 95 Hz and a period of 0 to 8.0 s. The plot represents an average across all subjects. First row represents *object* change, second row *location* change (second row), third row, object *or* location change, and fourth row, *location only* change which used a single color per trial.

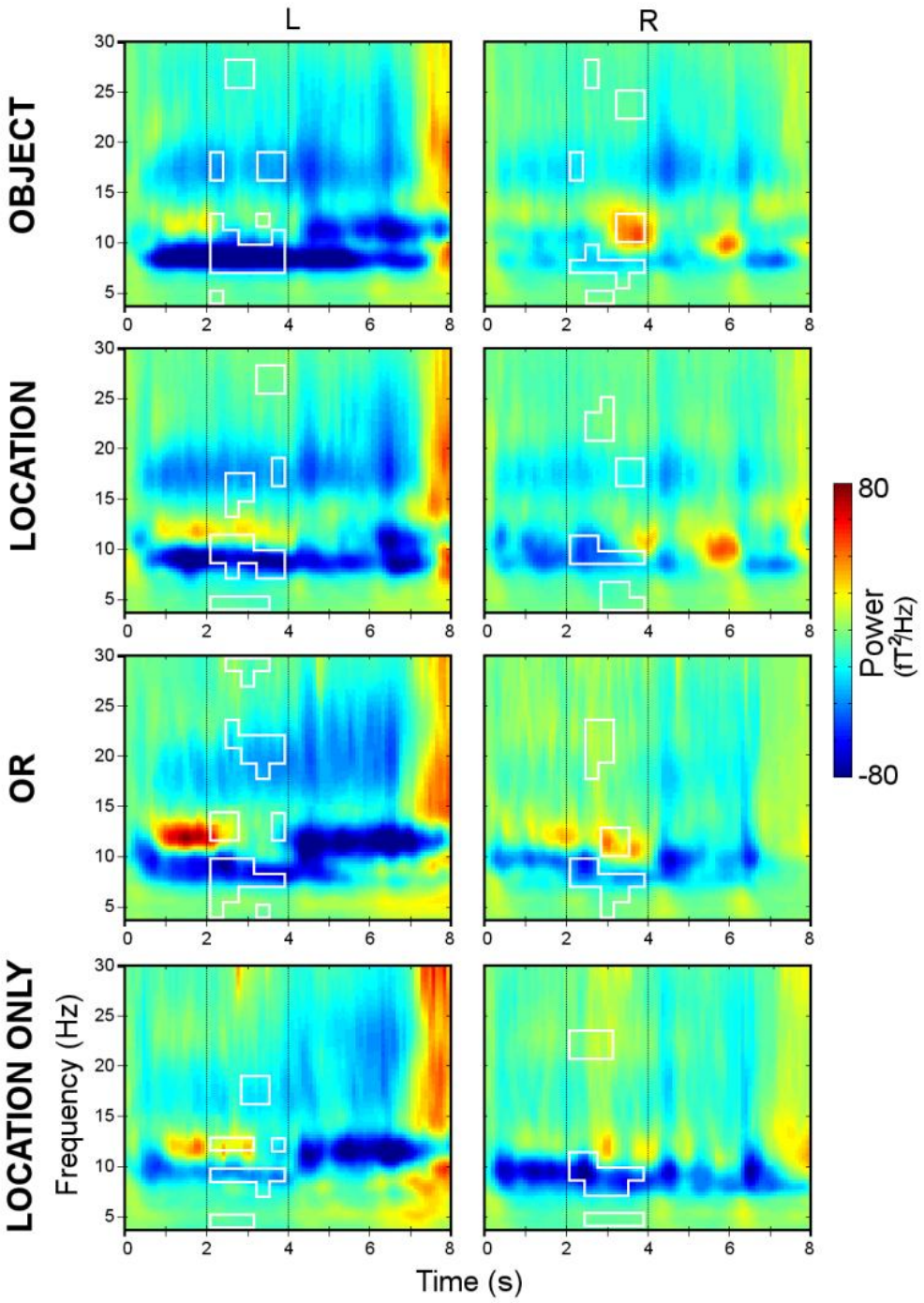

Figure 3.2 Time frequency plots (3 to 30 Hz)

Time-frequency plots from left and right MEG sensors covering the left and right lateral temporal regions, respectively, with a frequency range of 3 to 30 Hz and a period of 0 to 8.0 s. The plot represents an average across all subjects. White boxes indicate statistically significant spectra relative to baseline. Vertical black lines represent the beginning and end of the delay period. First row represents *object* change, second row, *location* change, third row, object *or* location change, and fourth row, *location only* change which used one color across items.

Figure 3.2 shows significant clusters of ERS and ERD in the frequency range extending from 3 Hz to 9Hz, which is roughly equivalent to the classically-defined theta range (4 to 8 Hz) compared to the other classically-defined ranges including alpha (8 to 13 Hz) and beta (13 to 30 Hz) ranges. Therefore, subsequent analyses of MEG data will focus on activity within the loose theta range (3 to 9 Hz) only. The study of this frequency range is in agreement with recently reported studies on VWM (e.g., Brookes et al., 2011). Accordingly, condition-specific topography of the power spectra at the sensor level were then computed within the theta range during the delay period (2 to 4 s post-trial onset) using a planar gradiometer representation (**Figure 3.3**). The planar field gradients were computed by estimating the gradients tangential to the scalp based on axial gradiometer signals. Typically, the signal amplitude is largest directly above a source when using a planar gradient transformation. Notice that the ERD observed across all conditions lies posteriorly over occipital and parietal regions bilaterally and anteriorly over frontal regions bilaterally. There is also a relatively weak ERS over medial frontal regions across all conditions.

While desynchronizations represent a decrease in oscillatory power at a given frequency range relative to baseline activity, the significance of this decrease relates to cognitive function. MEG studies have established a relationship between observed desynchronizations and various behaviors including language (e.g., Hirata et al., 2010; Passaro et al., 2011; Tavabi et al., 2011), memory (e.g., Brookes et al., 2011; Ciesielski et al., 2010; Grimault et al., 2009), and motor planning (e.g., Moses et al., 2010; Van Dijk et al., 2010;

Willemse et al., 2010). Accordingly, any statistically significant ERD observed in this study (**Figure 3.3**) will be considered equally among observed ERS across both spectral and source estimation techniques.

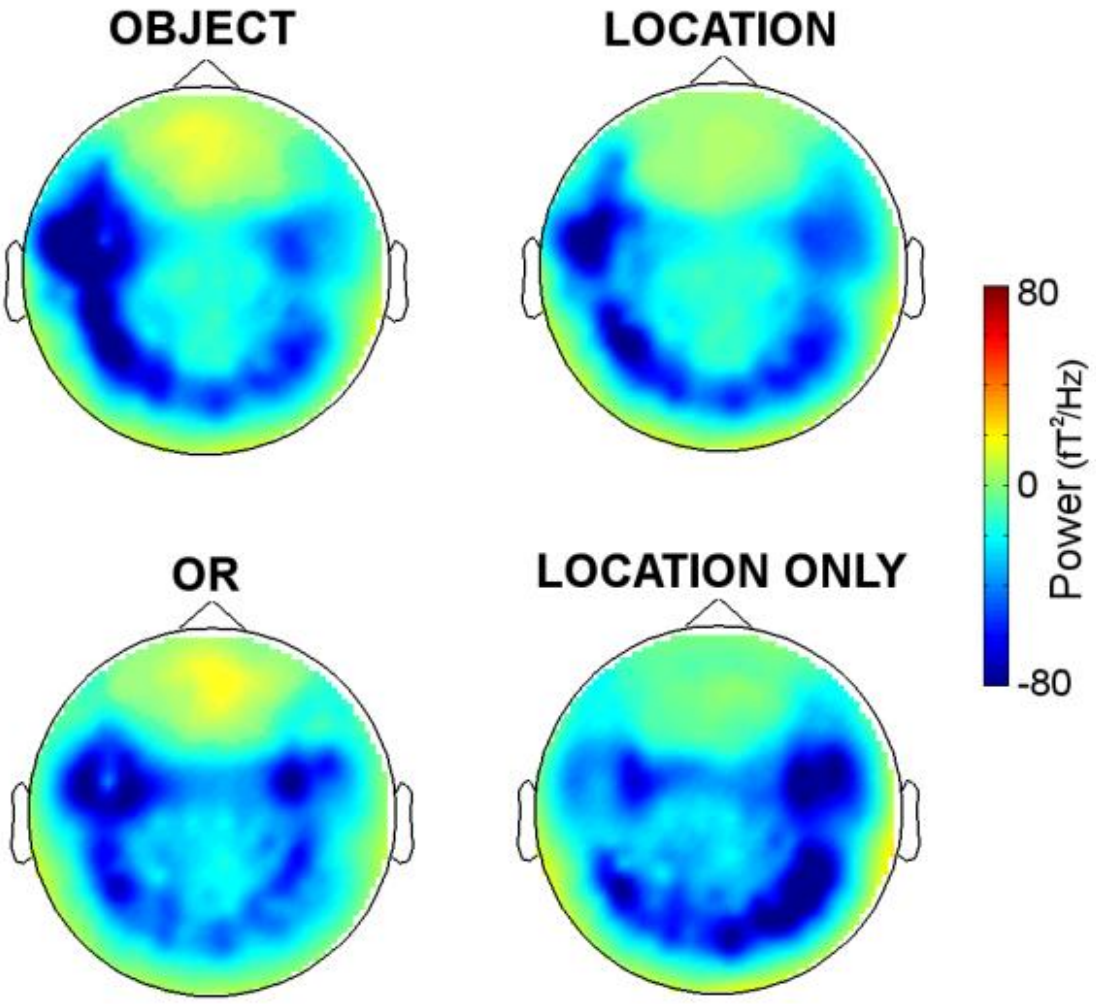

Figure 3.3 Topographical sensor plots (3 to 9 Hz)

Topographical sensor plots based on planar gradiometer representation. Topographies represent theta activity (3 to 9 Hz). Blue represents desynchronization and yellow represents synchronization relative to baseline. Top left: *object* change, top right: *location* change, bottom left: object *or* location change, bottom right: *location only* change which used one color across items.

Identifying the precise source of the biomagnetic signals recorded with MEG is impossible due to the inverse problem, but an approximation is possible through a distributed source, beamformer spatial filter. To estimate the sources corresponding to each condition, a frequency domain beamforming [dynamic imaging of coherent sources (DICS)] approach (Gross et al., 2001) was applied to the data on the basis of the time-frequency ranges selected from the spectral analysis (3 to 9 Hz). The DICS beamformer utilizes an adaptive spatial filter generated from the cross-spectral density matrix, which estimates the spatial distribution of power within a brain volume. The distribution relies on the amplitude at a specific frequency range recorded from all MEG sensors.

A statistical measure incorporating a dependent samples non-parametric statistical test was used to evaluate the reliability of the beamformer source localization for each subject. A post-stimulus time window (2000 ms to 4000 ms) was compared to the pre-stimulus window (-500 to 0 ms) across all trials. A Monte Carlo simulation of the pre- and post-stimulus data generating 1000 randomizations created a reference distribution of thresholded *t* statistics ($p < 0.05$). The test statistic comparing pre- and post-stimulus activity was derived on the basis of these thresholded *t* statistics. A spatial transformation to standard MNI space (International Consortium for Brain Mapping template, Montreal Neurological Institute, Montreal, Quebec) for each subject's MRI and the corresponding statistical source activity was applied using SPM2 (Statistical Parametric Mapping; http://www.fil.ion.ucl.ac.uk/spm).

To generate a time-course corresponding to the entire trial length, the MEG data was then split into 500 ms segments spanning the entire trial (8 s) and submitted to the spatial filter DICS beamformer on the basis of the frequency ranges selected from the spectral analysis (3 to 9 Hz) in **2.2**. The same source statistics and spatial transformation were applied using sixteen 500 ms windows from to 0 to 8 s post-trial onset to be compared with the pre-stimulus window (-500 to 0 ms pre-trial onset) across all trials. The results from this analysis were used for time-series plots within specified regions identified in the results

MEG Group Analysis

Group-level source maps of MEG data were computed for each condition using the same statistical approach applied at the subject-level. A cluster-based correction technique was implemented to correct for multiple comparisons on the basis of 1000 Monte Carlo simulations (Maris & Oostenveld, 2007). The group-level maps were then submitted to an independent-sample non-parametric *F* test to determine the main effect among the four conditions. The same cluster-based correction for multiple comparisons described above was applied. The resulting group maps on the basis of the *t* statistics and the main effect of condition as a result of the *F* test are projected on an inflated N27 brain.

3.3 RESULTS

In-Scanner Task Performance

Mean performance was above 80% across all four conditions in Experiment 2 as well (**Figure 3.4**): 83.9% ± 8.3 for the *object condition*, 84.4% ± 11.3 for the *location condition*, 85.8% ± 8.5 for the *or condition*, and 84.4% ± 11.3 for the *location only condition*. There was no significant difference between conditions on the basis of a one-way ANOVA [$F(3,36) = 0.57$, $p = 0.64$]. Mean response times across all four conditions are reported in **Figure 3.5.** Response times were between 800 and 900 ms across all four conditions and were not significantly different [$F(3,36) = 0.27$, $p = 0.85$]. Based on similar behavioral measures, the neural correlates associated with condition differences was known not to correspond to task difficulty across conditions

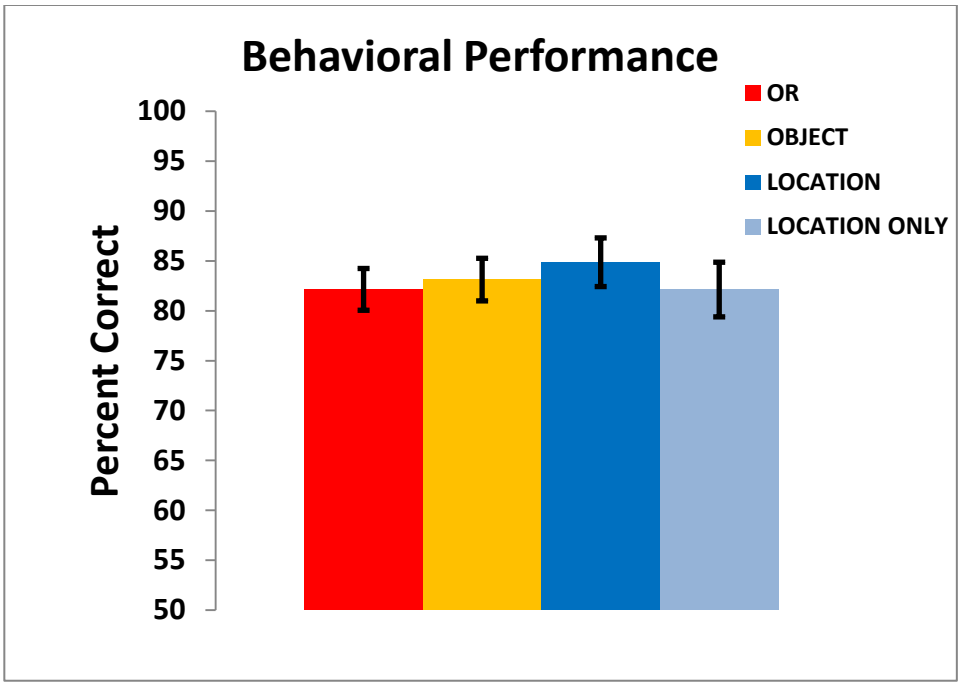

Figure 3.4 MEG Task Performance

Behavioral performance in the MEG scanner for each change detection condition. OR (red), object *or* location change; OBJECT (orange), object change; LOCATION (blue), location change; LOCATION ONLY (light blue), location only change which used a single color per trial.

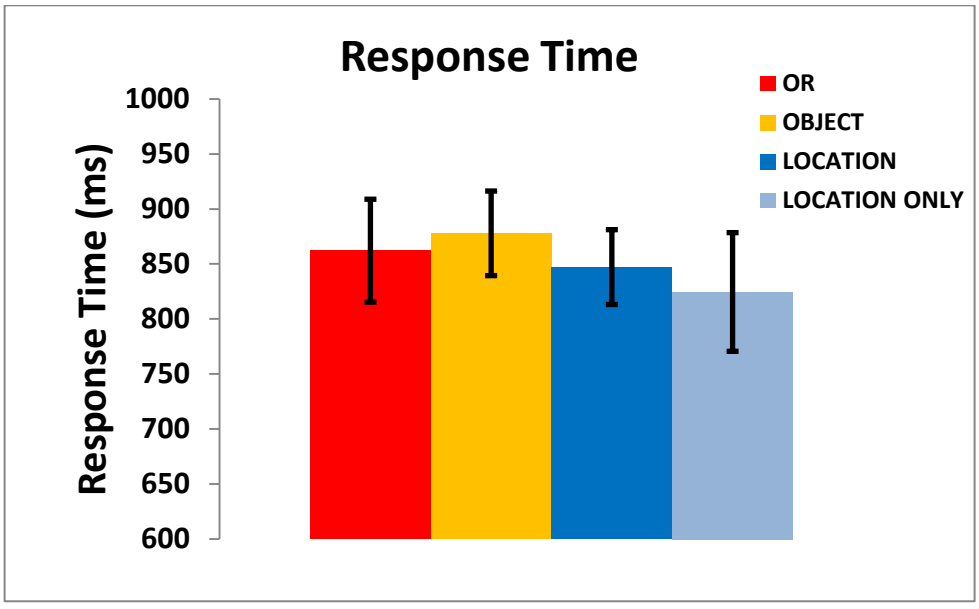

Figure 3.5 MEG Task Response Time

Response time in the MEG scanner for each change detection condition. OR (red), object *or* location change; OBJECT (orange), object change; LOCATION (blue), location change; LOCATION ONLY (light blue), location only change which used a single color per trial.

Brain Activation Profiles

Theta activation (3-9 Hz) during the delay period was observed in the form of ERD (blue) and ERS (red) bilaterally in frontal and parietal regions across CD conditions. Generally, ERD was observed in more posterior regions occupying occipital and parietal cortices as well as some posterior temporal regions. ERS was observed only in anterior medial regions in all conditions except for the *location only* condition (**Table 3.1**). A recent MEG study attempting to localize theta range activity for working memory tasks have identified a similar pattern of posterior ERD and anterior ERS (Brookes et al., 2011). In the case of the ERD, neural oscillations in the theta range decreased relative to baseline in the brain regions observed (**Figure 3.6**), which suggests an ERS has occurred in another higher or lower frequency range. In regards to the ERS, increases in the theta oscillations relative to baseline activity suggest the occurrence of an ERF in the regions observed in **Figure 3.6**.

ERD in parietal (IPL, SPL, and precuneus) and occipital (cuneus, middle occipital gyrus, and lingual gyrus) regions was observed in all four conditions, although it was less extensive in the *or condition*. The *location only* condition was the only condition which did not exhibit ERD localized to the left DLPFC (Ba 9). ERD in the paracentral lobule was found in the *location only* and *or* conditions while all but the *location only condition* exhibited ERD in the thalamus. All conditions exhibited some ERD in the left supramarginal gyrus, a region which has been identified as an area responsible for establishing language laterality based on ERD (e.g., Passaro et al., 2011). ERD localized to the left inferior

frontal gyrus (Ba 47) extending to the superior temporal gyrus (STG) was found in all but the *or condition*. Finally, the *location only* condition was the only condition with ERD located in the right medial frontal gyrus (Ba 11) and anterior cingulate.

As mentioned earlier, ERS was observed in all conditions except for the *location only condition*. ERS was observed in more medial prefrontal regions including Ba 10 in the right hemisphere and Ba 9 medially in all three conditions. Additionally, the *or* and *object* conditions evoked an ERS in the left Ba 10 region. Only the *object condition* demonstrated an ERS in the anterior cingulate and Ba 10 medially.

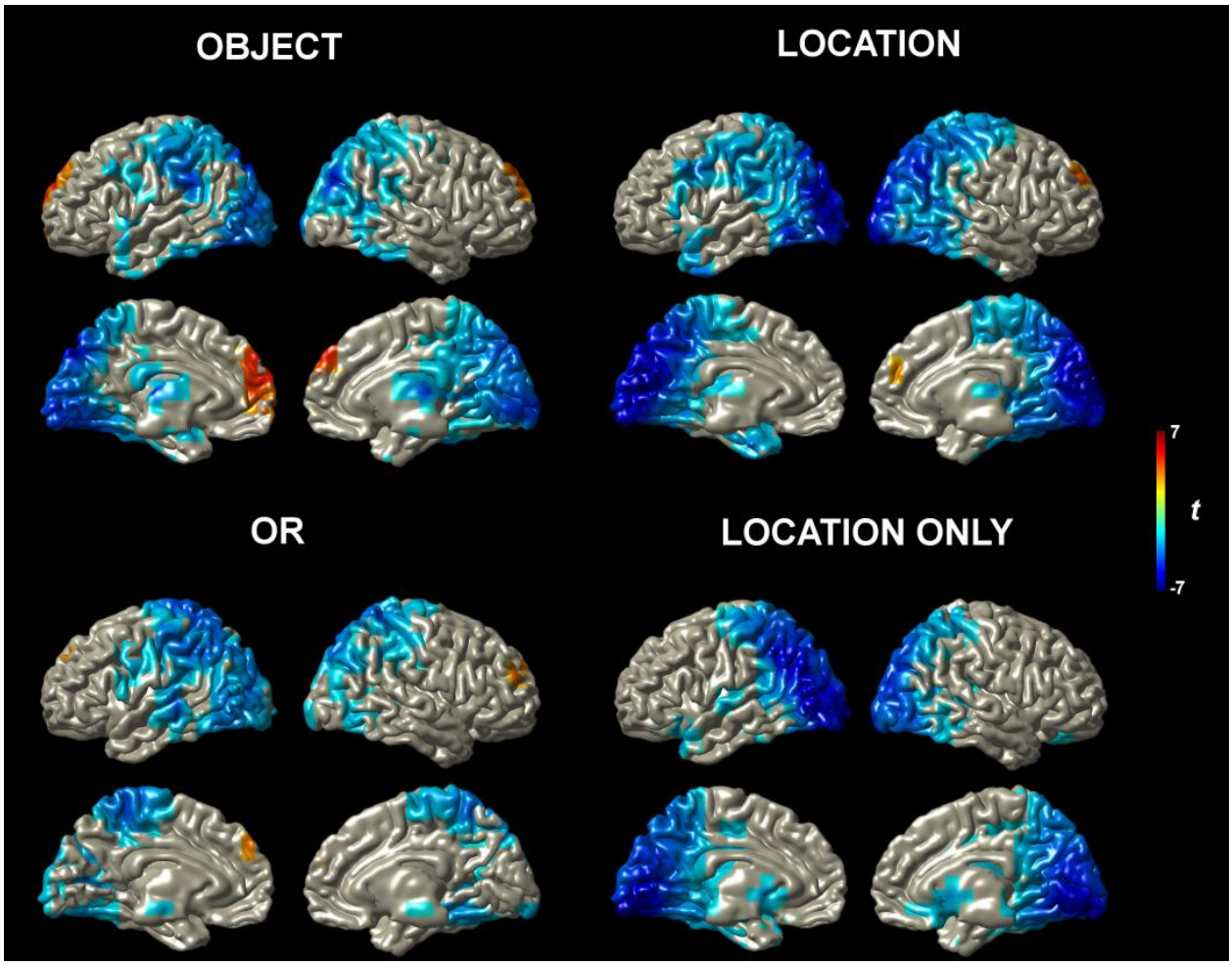

Figure 3.6 Group activation maps for each change detection condition

Statistically significant group activation maps (corrected $p < 0.05$) for each change detection condition. Top left: *object* change, top right: *location* change, bottom left: object *or* location change, bottom right: *location only* change which used a single color per trial.

Condition	ERS/ERD	Brain Region	BA	Hem.	X	y	z	*t*-value
Object	ERS	medial frontal gyrus, superior frontal gyrus, middle frontal gyrus, anterior cingulate	10	L+R	8.0	50.0	40.0	5.202
	ERD	superior parietal lobule, inferior parietal lobule, precuneus	19	R	-10.0	-84.0	46.0	-5.985
		superior parietal lobule, precuneus	19	L	38.0	-80.0	32.0	-5.143
		cuneus, lingual gyrus	17	L+R	4.0	-96.0	-4.0	-4.601
		fusiform gyrus, middle occipital gyrus	37	L	-40.0	-74.0	-16.0	-3.983
		insula, superior temporal gyrus, temporal pole	13	L	-42.0	10.0	2.0	-3.398
		inferior temporal gyrus	20	L	-50.0	-26.0	-24.0	-3.106
		fusiform gyrus, inferior temporal gyrus	37	R	54.0	-30.0	-26.0	-3.167
		supramarginal gyrus, superior temporal gyrus	22	R	58.0	-38.0	34.0	-2.986
		inferior parietal gyrus, supramarginal gyrus, superior temporal gyrus	40	L	-60.0	-38.0	32.0	-4.493
		middle frontal gyrus, inferior frontal gyrus	9	L:	-52.0	6.0	38.0	-2.936
		thalamus		L+R	4.0	-20.0	8.0	-4.480
		posterior cingulate	23	L+R	2.0	-62.0	14.0	-2.817
Location	ERS	superior frontal gyrus, middle frontal gyrus, medial frontal gyrus	10	R	20.0	50.0	30.0	4.095
	ERD	cuneus, middle occipital gyrus, lingual gyrus	19	L	-30.0	-82.0	14.0	-7.020
		cuneus, middle occipital gyrus, lingual gyrus	19	R	10.0	-99.0	20.0	-8.560
		precuneus, superior parietal lobule, inferior parietal lobule	19	L	-28.0	-68.0	40.0	-5.092
		inferior parietal lobule, precuneus, superior parietal lobule	40	R	42.0	-64.0	40.0	-5.143
		middle frontal gyrus, inferior frontal gyrus	9	L	-52.0	12.0	38.0	-3.570
		inferior frontal gyrus, superior temporal gyrus, temporal pole	47	L	-52.0	18.0	0.0	-2.971
		fusiform gyrus, inferior temporal gyrus	37	L	-48.0	-52.0	-16.0	-3.982
		fusiform gyrus, inferior temporal gyrus	37	R	52.0	-60.0	-16.0	-3.438
		thalamus		L+R	2.0	-18.0	10.0	-3.202
		posterior cingulate, paracentral lobule, cingulate	30	L+R	-2/0	-52.0	18.0	-3.697
Or	ERS	middle frontal gyrus, superior frontal gyrus	10	R	30.0	60.0	20.0	4.037
		medial frontal gyrus	10	L+R	-4.0	62.0	18.0	3.565
		superior frontal gyrus	9	L	-22.0	50.0	38.0	3.166
	ERD	superior parietal gyrus, inferior parietal gyrus, postcentral gyrus, middle occipital gyrus, superior occipital gyrus, paracentral lobule	7	L	-20.0	-56.0	66.0	-4.744
		superior parietal gyrus, inferior parietal gyrus, postcentral gyrus, paracentral lobule	7	R	18.0	-50.0	62.0	-4.398
		supramarginal gyrus, inferior parietal lobule, superior temporal gyrus	40	L	-50.0	-38.0	40.0	-4.363
		cuneus, lingual gyrus	18	L+R	0.0	-98.0	-6.0	-3.347
		middle occipital gyrus	19	R	32.0	-80.0	20.0	-2.949
		middle temporal gyrus, superior temporal gyrus	22	L	-68.0	-26.0	0.0	-3.498
		inferior frontal gyrus, middle frontal gyrus, precentral gyrus	9	L	-62.0	10.0	28.0	-3.012
		fusiform gyrus, middle occipital gyrus	19	L	-54.0	-70.0	-16.0	-3.429
		fusiform gyrus, middle occipital gyrus	19	R	48.0	-68.0	-16.0	-2.901
		thalamus, red nucleus		L+R	8.0	-12.0	-2.0	-3.272
Location Only	ERD	cuneus, lingual gyrus, middle occipital gyrus, inferior occipital gyrus	18	L+R	-14.0	-92.0	-16.0	-6.832
		superior parietal lobule, precuneus, cuneus, middle occipital gyrus	7	R	26.0	-76.0	44.0	-5.264
		superior parietal lobule, inferior parietal lobule, precuneus, cuneus, middle occipital gyrus	7	L	-42.0	-68.0	44.0	-5.312
		Inferior parietal lobule	40	R	42.0	-36.0	34.0	-3.169
		fusiform gyrus, inferior temporal gyrus	37	L	-46.0	-64.0	-20.0	-3.359
		fusiform gyrus, inferior temporal gyrus	37	R	52.0	-56.0	-20.0	-3.121
		posterior cingulate gyrus, cingulate gyrus	31	L+R	2.0	-52.0	26.0	-3.219
		inferior frontal gyrus, superior temporal gyrus	47	L	-48.0	18.0	-10.0	-3.286
		superior temporal gyrus, middle temporal gyrus	22	L	-60.0	-16.0	0.0	-2.789
		medial frontal gyrus, anterior cingulate	11	R	14.0	36.0	-10.0	-2.856
		caudate, putamen		L+R	6.0	10.0	-2.0	-2.736

Table 3.1 Cluster analysis for each change detection condition

Clusters of activation are significant at a corrected $p < 0.05$. Hem = hemisphere; L= left, R = right, L+R = a single cluster across hemispheres. Talairach coordinates correspond to peak activation within a cluster.

The main effect associated with the four MEG conditions are illustrated in **Figure 3.7**. Accordingly, the analysis yielded six clusters which demonstrated a main effect across conditions (**Table 3.2**). Time-courses associated with each condition are illustrated in **Figure 3.7a - 3.7f**. Time points are represented every 500 ms in order to take advantage of the temporal resolution afforded by MEG.

The medial view of **Figure 3.7** (bottom row) shows two clusters, one in the anterior cingulate (AC) and Ba 10, and the other in the cuneus (CUN) and precuneus (PCUN). The anterior cingulate corresponds to an object greater-than location gradation in the form of an ERS whereby the *object* and the *or* conditions are significantly greater than the *location* and *location only* conditions (**Figure 3.7a**). Conversely, a gradient in favor of the location conditions is observed in the cuneus/precuneus cluster of activation (**Figure 3.7b**). Clusters in the left DLPFC (**Figure 3.7e**), the right Ba 10 (**Figure 3.7d**), and to a some extent in the right Ba 11 (**Figure 3.7c**), appear to exhibit profiles of activation across conditions in favor any condition involving more than one identity within a stimulus display. As the *location only* condition presented a uniform color for each display, items could only be distinguished on the basis of location. Therefore, differences across conditions which show a greater ERS or ERD in favor of all but the *location only* conditions must represent some object identity component even if the condition did not explicitly require subjects to remember such information. Finally, the cluster corresponding to the left ITG shows a greater ERD for *location* and *location only* condition compared to *object* and *or* conditions (**Figure 3.7f**).

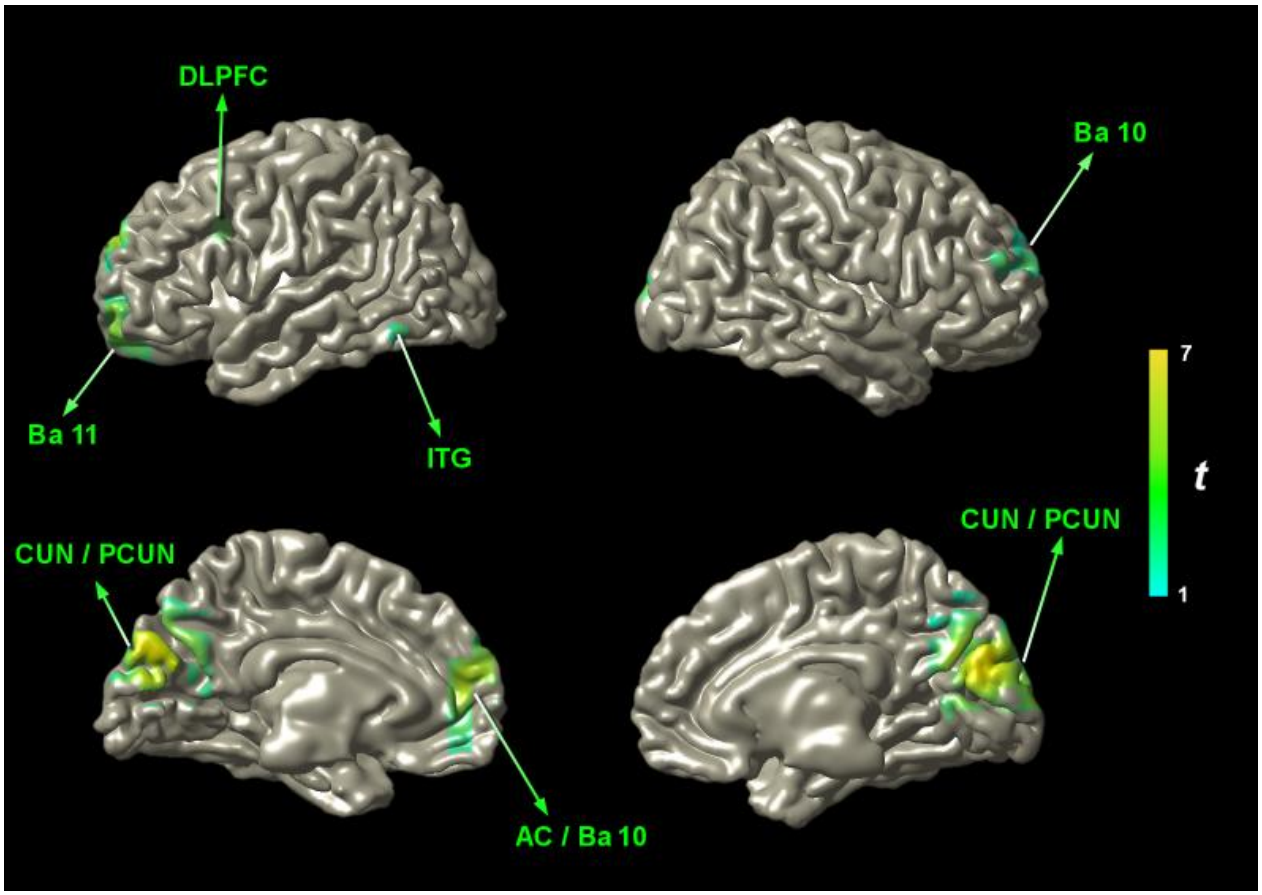

Figure 3.7 Main effect of MEG task condition

Group activation map of main effect of neural activity across change detection conditions. Activations are significant at a corrected $p < 0.05$. Labeled regions: DLPFC, dorsolateral prefrontal cortex; ITG, inferior temporal gyrus; Ba 11, Brodmann area 11; Ba 10, Brodmann area 10; AC, anterior cingulate; CUN, cuneus; PCUN, precuneus.

Brain Region	BA	Hemisphere	x	y	z	*t*-value
cuneus, precuneus	18	L+R	0.0	-76.0	29.0	6.941
anterior cingulate, medial frontal gyrus	10	L+R	-10.0	45.0	4.0	5.645
inferior temporal gyrus	37	L	-59.0	-60.0	-5.0	4.319
middle frontal gyrus, inferior frontal gyrus	9	L	-58.0	2.0	-23.0	3.712
Superior frontal gyrus, middle frontal gyrus	11	L	-26.0	59.0	-13.0	5.114
middle frontal gyrus, superior frontal gyrus	10	R	35.0	53.0	21.0	3.985

Table 3.2 Cluster analysis of main effect

Clusters of activation represent main effect across change detection conditions and are significant at a corrected $p < 0.05$. L= left hemisphere, R = right hemisphere, L+R = a single cluster extending from one hemisphere to the other. Talairach coordinates correspond to peak activation within a cluster.

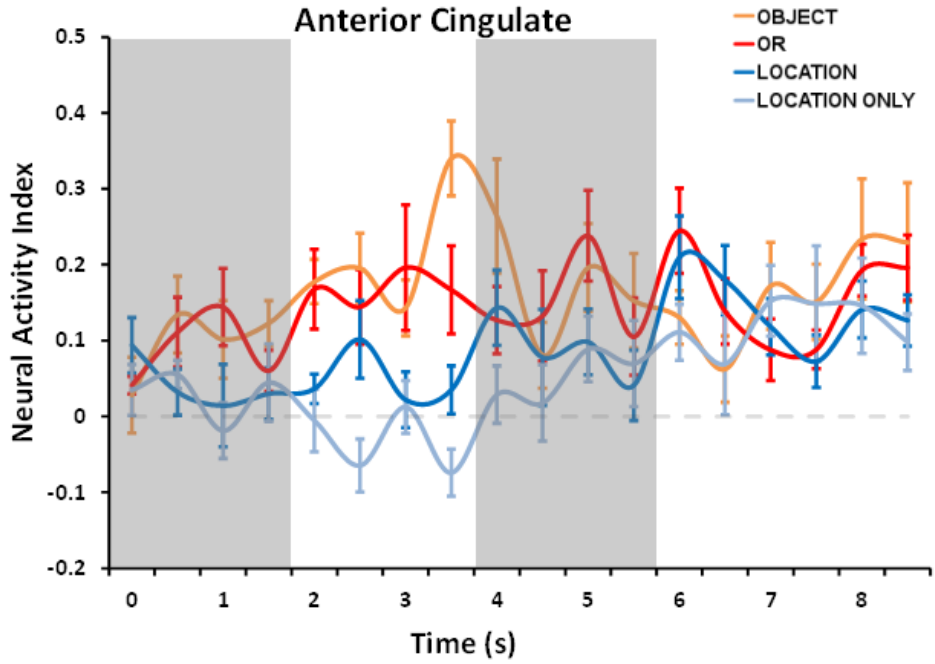

Figure 3.7a Anterior cingulate time-course

Time-courses of neural oscillations (3-9 Hz) within the anterior cingulate activation from Figure 3.7. Error bars represent standard errors of the mean. Gray bars indicate sample and test periods respectively.

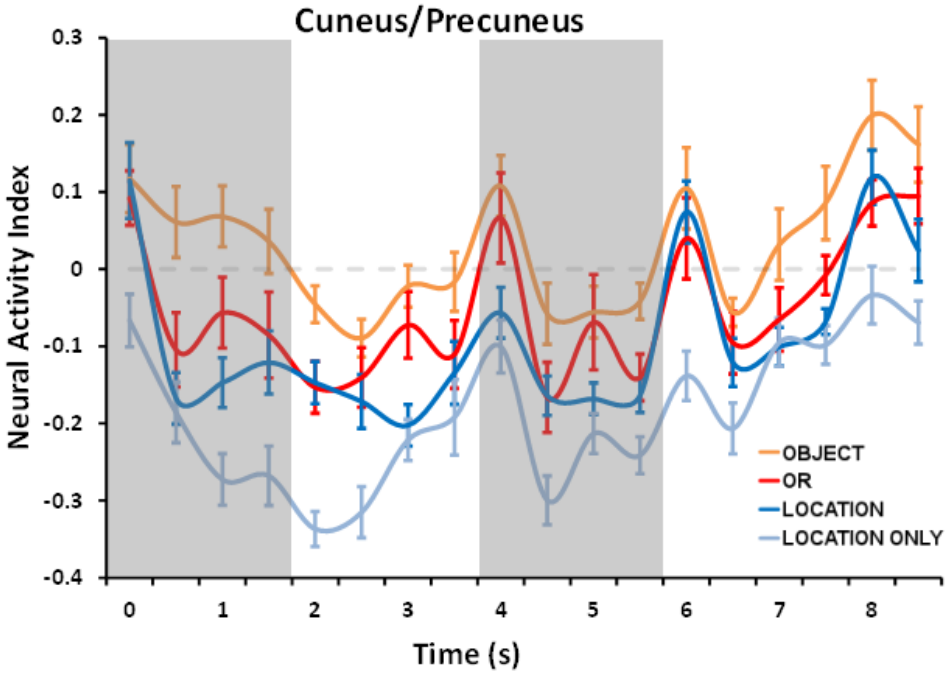

Figure 3.7b Cuneus/Precuneus time-course

Time-courses of neural oscillations (3-9 Hz) within the cuneus/precuneus activation from Figure 3.7. Error bars represent standard errors of the mean. Gray bars indicate sample and test periods respectively.

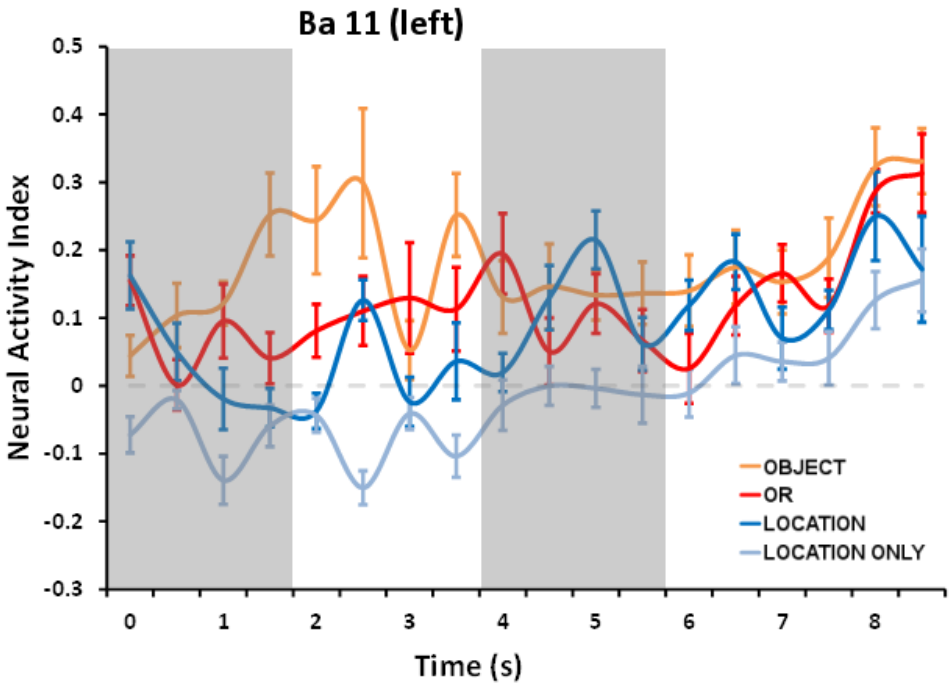

Figure 3.7c Left Ba 11 time-course

Time-courses of neural oscillations (3-9 Hz) within the left Ba 11 activation from Figure 3.7. Error bars represent standard errors of the mean. Gray bars indicate sample and test periods respectively.

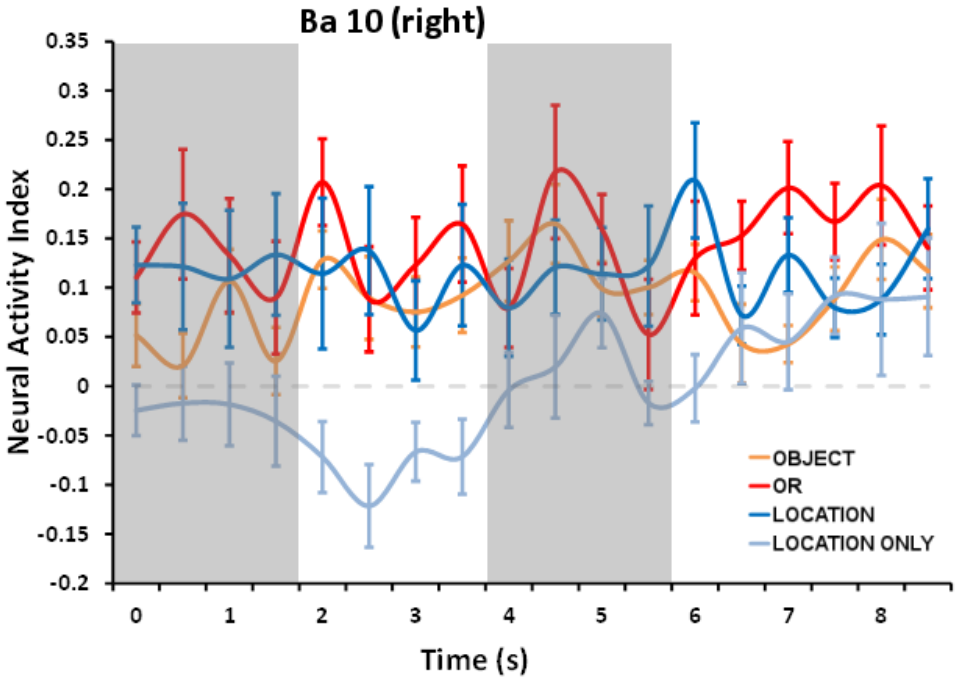

Figure 3.7d Right Ba 10 time-course

Time-courses of neural oscillations (3-9 Hz) within the right Ba 10 activation from Figure 3.7. Error bars represent standard errors of the mean. Gray bars indicate sample and test periods respectively.

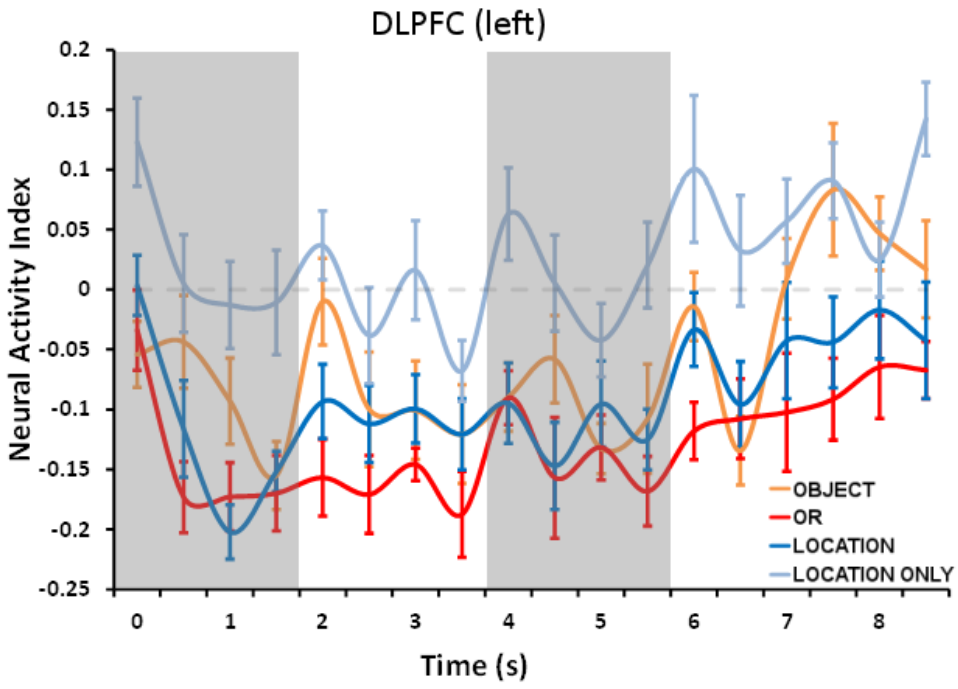

Figure 3.7e Left DLPFC 10 time-course

Time-courses of neural oscillations (3-9 Hz) within the left DLPFC activation from Figure 3.7. Error bars represent standard errors of the mean. Gray bars indicate sample and test periods respectively.

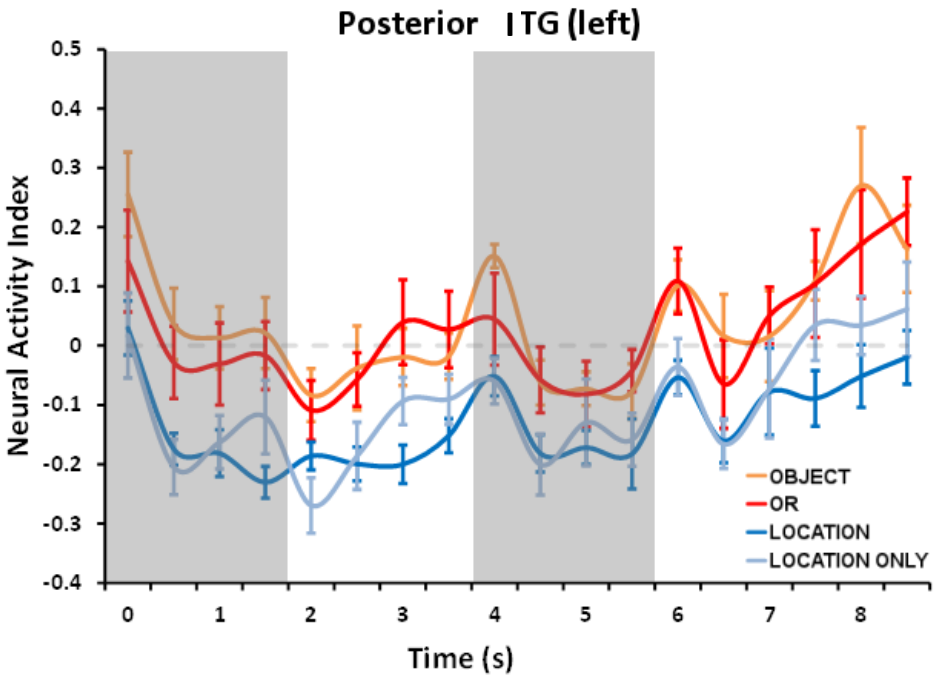

Figure 3.7f Left ITG time-course

Time-courses of neural oscillations (3-9 Hz) within the left posterior ITG activation from Figure 3.7. Error bars represent standard errors of the mean. Gray bars indicate sample and test periods respectively.

3.4 DISCUSSION.

The aims of this experiment were: (1) identify and localize the frequency range of activity corresponding to the delay period of VWM, (2) demonstrate a dissociation of object-location VWM, and (3) determine if the results corresponded to a caudal-rostral or a dorsal-ventral interpretation of VWM dissociation . A theta range (3-9 Hz) was identified as the frequency range among all other tested ranges which demonstrated a greater number of significant spectra (oscillatory power) as compared to baseline. This is in agreement with a recently published study by Brookes et al. (2011) which analyzed all frequency ranges (up to 100 Hz) and determined that only the theta range exhibited statistically significant increases corresponding to working memory during the maintenance period. Furthermore, ERS within this frequency range was shown to increase with increased memory load. Activity associated with the theta range was localized to posterior (parietal and occipital) and prefrontal regions across conditions, also in agreement with MEG and EEG VWM literature studying theta range activity (e.g., Brookes et al., 2011; Meltzer et al. 2008; Scheeringa et al., 2009).

Theta Activity

The EEG literature studying various frequency ranges in the context of VWM have consistently identified the theta and alpha bands as significant frequency ranges of interest. An early review by Klemish et al. (1997) identified the ERS in the upper alpha range as a component which negatively correlated

with memory performance. Conversely, the theta range ERS was shown to correlate positively with memory performance across studies. Later EEG studies found convergent evidence supporting a positive relationship between theta ERS and working memory performance (Bastiaansen et al., 2002; Doppelmayr et al., 1998; Düzel et al., 2003; Krause et al., 2000; Li et al., 2011; Meltzer et al. 2008; Mizuhara et al., 2011; Scheeringa et al., 2009). Only a few MEG studies have shown a similar relationship between theta oscillations and working memory performance during the delay period (Brookes et al., 2011; Jensen & Tesche,2002; Onton et al., 2005).

The observed increase in theta activity (as an ERS) observed across EEG and MEG studies has been consistently localized to prefrontal regions. In particular, source estimation techniques across imaging modalities have localized theta ERS to medial prefrontal cortices and in some cases, in the anterior cingulate cortex (Asada et al., 1999; Brookes et al., 2011; Ishii et al., 1999; Jensen et al., 2002; Li et al., 2011; Mizuhara et al., 2011). Our results showed localized theta ERS in the prefrontal cortex (**Figure 3.6**) and are consistent with these findings. Interestingly, only the *location only* condition did not evoke an ERS in prefrontal regions or any other brain region for that matter. This suggests that among healthy individuals, unique identities among simultaneously-presented items are required in order to evoke an ERS in the theta range, regardless of the memory task objective (location, object, or both). This finding in the context of a VWM task is reported here for the first time and should be studied in further detail especially in the context of memory workload

which has been shown to positively correlate with ERS in prefrontal regions (e.g., Brookes et al., 2011).

Only a few EEG and MEG studies have reported theta ERD in posterior regions similar to the findings reported here (**Figure 3.6**). In particular, only one EEG study by Meltzer et al. (2008) has reported ERD during the maintenance period of a VWM task. Furthermore, only a few MEG studies have reported posterior ERD activity within the theta range (Brookes et al., 2011; Jensen & Tesche,2002; Onton et al., 2005). These studies utilized a form of time-frequency analysis which compares theta oscillations to baseline activity and thus allows for the detection of both positive (ERS) and negative (ERD) activity. Many of the earlier EEG studies which reported on theta oscillations, performed a simple Fourier or wavelet analysis on the post-stimulus signal only. However, several EEG studies which compared the post-stimulus signal to baseline (pre-stimulus signal) and reported an ERD in other frequency ranges, namely the alpha band, did not report a posterior theta ERD (Düzel et al., 2003; Li et al., 2011; Scheeringa et al., 2009). While it is unclear why such an ERD was not detected in these studies, several factors including task design and timing, statistical analysis, and the choice for baseline activity may produce varying results in time-frequency analyses across studies. While posterior theta ERD has not been shown to correlate with either memory performance or workload, it has been reported as a statistically significant source of activity as compared to baseline across studies (Brookes et al., 2011; Jensen & Tesche,2002; Meltzer et al., 2008; Onton et al., 2005).

Location and Object Identity VWM Dissociation Using MEG

Only one MEG study has explored VWM in the context of object and location memory (Jokisch & Jensen, 2007) and the focus was on posterior occipital regions. Therefore, results from our experiment described here will be compared to findings in the fMRI literature. The anterior cingulate and medial frontal gyrus along with the left orbital gyrus (Ba 11) were the primary loci responsible for greater object ERS compared to location ERS. A recent study by Harrison et al. (2010) identified the main effects of object and location memory and found activation in the left orbital gyrus to correspond to object memory only. This region is similar to the one reported here with MEG showing a similar object greater than location relationship. Several early fMRI and PET studies demonstrated activation corresponding to object memory in the anterior cingulate cortex (Haxby et al., 1995; Petrides et al., 1993). However, such a finding was not reported in more recent studies of object and location WM. Based on recent studies comparing MEG and fMRI, theta band activity has been shown to negatively correlate with BOLD in medial prefrontal regions (Michels et al., 2010; Scheeringa et al., 2008). In light of this finding, it is likely that previous fMRI studies did not report a difference in negative BOLD relative to baseline which may produce convergent results with those reported here in the medial prefrontal regions.

The object-location dissociation observed within the cuneus and precuneus in favor of an object greater-than location ERD has not been previously reported in the literature. Although, fMRI studies have implicated this

region in location WM tasks based on comparisons of BOLD profiles between object and location memory conditions (e.g., Borowsky et al., 2005; Mohr et al., 2006; Sala & Courtney, 2007). Similarly, BOLD signals in favor of location memory compared to object memory has been identified in the posterior ITG/MTG region (e.g., Borowsky et al., 2005; Mohr et al., 2006) as reported here (**Figure 3.7f**). Comparisons between fMRI findings on VWM and the MEG findings reported here demonstrate convergent results across imaging methods which record different components of the neural signal. Accordingly, these MEG findings contribute to the VWM literature by providing a finer temporal resolution than is currently possible with fMRI and thus allowing for the detection of differences among location and object neural oscillations.

A Caudal-Rostral Interpretation Using MEG

In this experiment, the main effect of CD conditions revealed several loci of location and object identity VWM dissociation. Specifically, rostral regions, including the anterior cingulate, the DLPFC, Ba 10, and Ba 11, exhibited greater amplitude (ERD or ERS) for identity memory conditions and conditions with multiples object identities. Conversely, a rostral region within the cuneus and precuneus demonstrated greater activity for location memory conditions. Taken together, these results do not follow a dorsal-ventral framework of location and object identity memory dissociation. Instead, a caudal-rostral interpretation of memory dissociation, similar to that observed in the fMRI experiment, is apparent in these findings. Accordingly, these results provide convergent evidence with the findings from the fMRI experiment, which also suggest a location-object

dissociation within a caudal-rostral framework rather than the commonly suggested dorsal-ventral framework.

CHAPTER 4

DISCUSSION AND CONCLUSIONS

4.1 Discussion

The brain regions and networks underlying location and object identity memory have yet to be robustly elucidated. Theoretically, it should be possible to dissociate brain networks responsible for the maintenance of locations and object identities using a well-controlled experiment that employs identical stimulus and task parameters. This was the objective of the first experiment (**Chapter 2**) which utilized a CD paradigm and fMRI to identify a functional separation associated with location and object identity memory networks. Similarly, the dissociation of location and object identity memory using the same change detection tasks and MEG was the objective of the second experiment (**Chapter 3**). These two experiments successfully addressed the first objective of this study. Furthermore, results from both experiments suggested a preponderance of activation corresponding to location and object identity memory extending from caudal to rostral regions, respectively, thus addressing the third primary objective of this project. To address these objectives, we directly compared four CD conditions. A main effect of conditions was observed in both fMRI and MEG methods which appear to suggest a caudal-rostral dissociation corresponding to location and object memory, respectively. Across conditions and imaging modalities, no dorsal-ventral location-object memory separation was observed in the prefrontal cortex (or in any other area) which is in disagreement with previous neuroimaging studies (e.g., Courtney et al., 1996; Jokisch & Jensen, 2007; Sala & Courtney, 2007), although findings from these and other studies present similar results which are in favor of a caudal-rostral dissociation.

Findings from the fMRI experiment identified several areas activated during the delay period. A single rostral region, occupying the left posterior portion of DLPFC (Ba 9), was significantly more active during the object identity condition than the location condition during the delay period. Conversely, a caudal region located in the right IPL was significantly more active during the location change condition than the object identity condition. Moreover, bilateral LOC activation was greater for location than object identity maintenance. These findings were in accordance with the proposed caudal-rostral separation of location and object identity memory. Finally, the left fusiform gyrus showed greater activation during object identity memory as compared to location memory while the right fusiform gyrus showed greater activation for the *location only* condition as compared to all other conditions. With the exception of fusiform activity, results from this experiment suggest a caudal-rostral dissociation for location and object identity VWM, respectively.

The MEG experiment utilized the same CD conditions and task parameters set forth in the fMRI experiment. Results from MEG showed a separation, caudally, in favor of location memory over object memory in a diffuse medial region extending from the cuneus to the precuneus bilaterally. Conversely, a cluster of activation rostrally, in the anterior cingulate and Ba 10 bilaterally, produced greater object than location activation. Several other rostral regions exhibited a dissociation of greater activation for conditions involving object information, although not necessarily requiring the memory of such information including the left DLPFC and a region occupying the right Ba 11. The

left Ba 11 cluster of activation exhibited a similar dissociation of object greater-than location amplitude as demonstrated by the dissociation in the anterior cingulate. Finally, a separation of location greater-than object memory was found in a caudal region occupying the left posterior ITG. The regions of location and object memory dissociation identified in this MEG experiment suggest a caudal-rostral dissociation of object and location memory.

The primary hypothesis of this project posits a dissociation of location and object identity memory with caudal regions corresponding more to location memory and rostral regions corresponding more to object identity memory. Findings from both the fMRI and MEG experiments concur with this hypothesis.

The change detection (CD) paradigm utilized in this study requires subjects to maintain visual information associated with at least five items in order to provide a correct response. While six items are presented during the stimulus display, only one item will change in the test display which follows the delay, thus requiring the subject to remember only five items as it may be assumed that the sixth item had changed if all other items remain the same. As all four task conditions make use of a 6-item display, the subsequent imaging analysis should yield active brain regions in areas associated with VWM. Conversely, if the task demands are great, either nothing is stored in memory during the delay or brain regions are engaged which are not normally associated with VWM but become active in order to compensate for task difficulty. Therefore, the aim is to achieve performance within the 80-90% range in order to prevent the task from being too difficult while also maximizing VWM capacity. Accordingly, performance across

all four conditions and both imaging modalities was similar and corresponded to the 80% criterion (**Figure 4.1**)

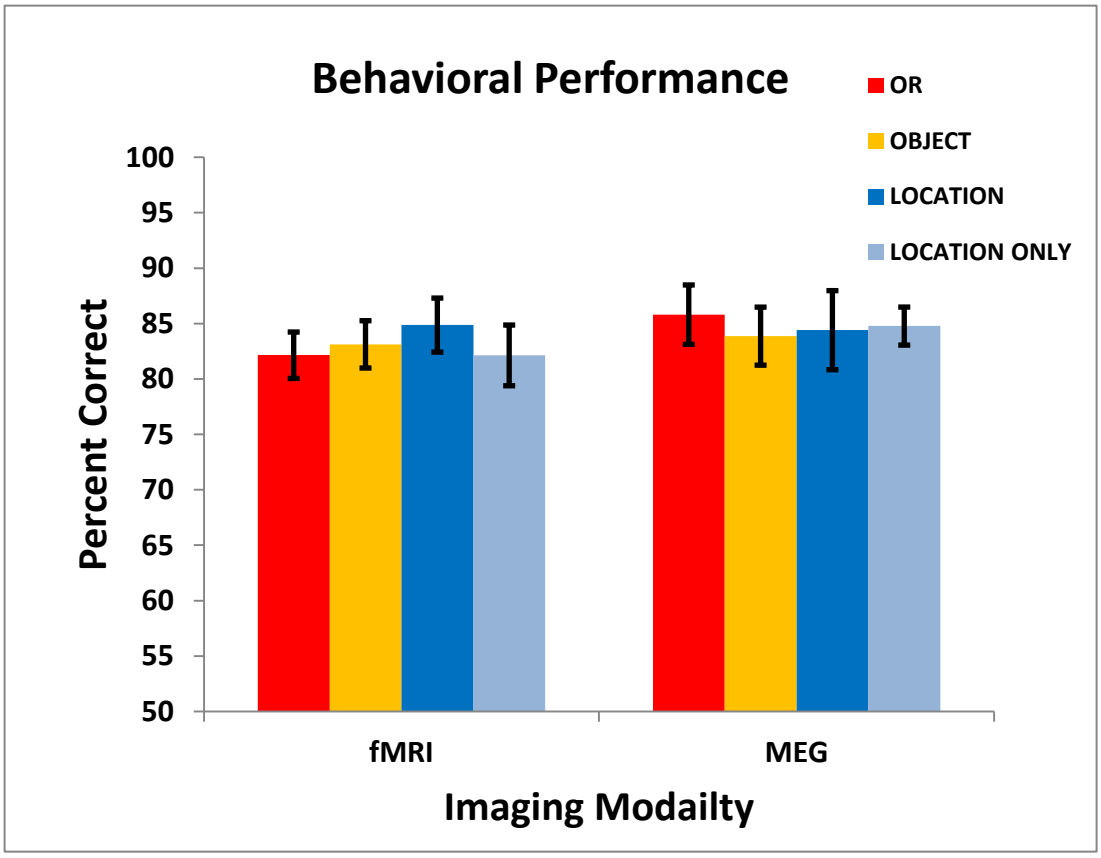

Figure 4.1 fMRI and MEG Task Performance

Behavioral performance in the fMRI and MEG scanners for each change detection condition. OR (red), object *or* location change; OBJECT (orange), object change; LOCATION (blue), location change; LOCATION ONLY (light blue), location only change which used a single color per trial.

While MEG and fMRI measure different components of the neural signal, both directly and indirectly, we explored the relationship between these techniques. To further elucidate this relationship, a re-analysis of these data is presented here to show how these measures vary with behavioral task performance. Individual performance during the object identity condition was correlated with the activation profiles of MEG and fMRI separately using a simple

Pearson's correlation to test for a linear relationship. The voxels obtained from the fMRI analysis which produced a significant correlation ($p < 0.05$; $df = 8$) are illustrated in **Figure 4.2**. Similarly, the profile of correlated voxels for the MEG experiment is illustrated in **Figure 4.3**. To correct for spurious voxels which might have exhibited a significant correlation, a cluster analysis was employed with a threshold of 12 contiguous voxels per cluster. Regarding the MEG data which contained both positive and negative values, only those voxels which demonstrated a positive correlation between performance and the absolute value of the localized source are reported. Similarly, only voxels from the fMRI analysis which exhibited a positive correlation with performance are reported. Correlated regions which overlap across these two methods are labeled accordingly.

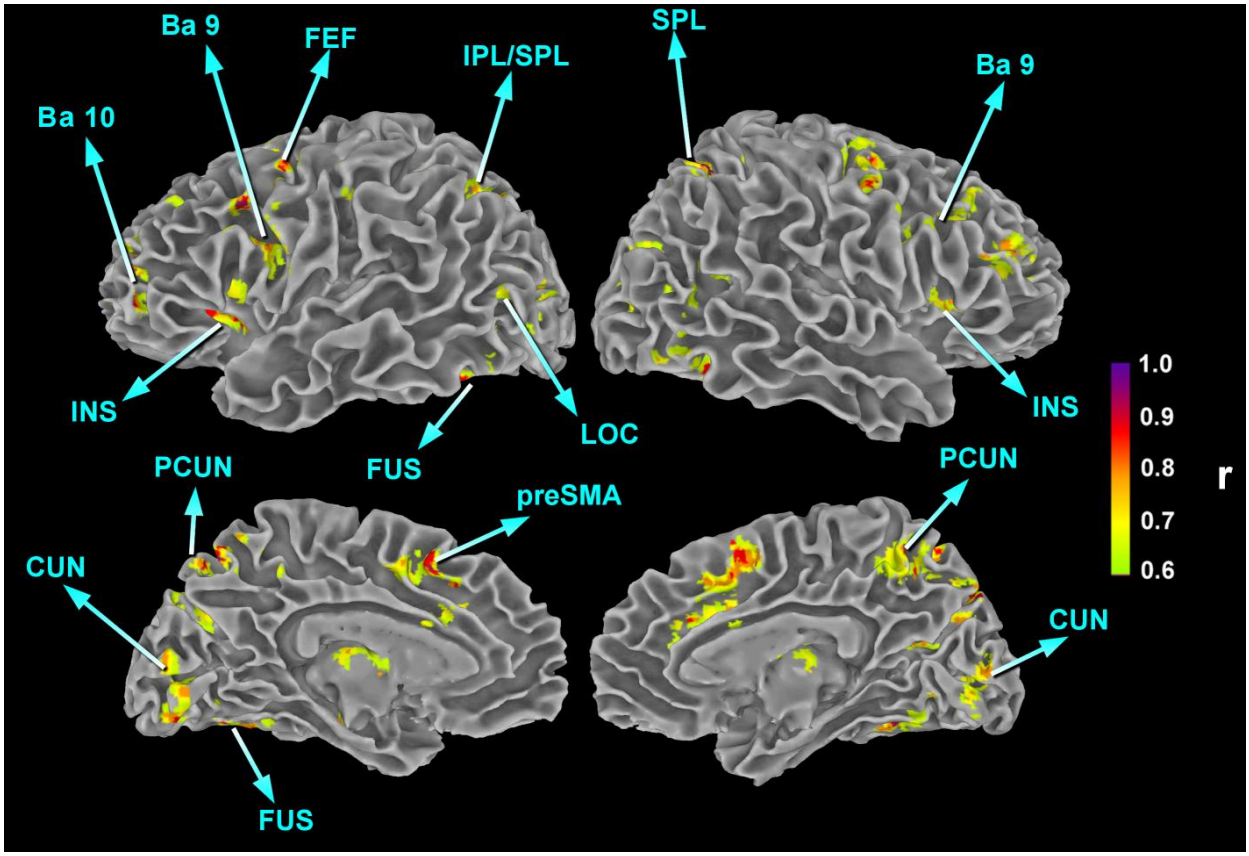

Figure 4.2 fMRI neural activity correlated with performance

Neural activity from fMRI experiment correlated with performance across subjects for *object* change conditions. Correlations are significant at $p < 0.05$. Labeled regions: Ba 10, Brodmann area 10; Ba 9, Brodmann area 9; FEF, frontal eye field; IPL, inferior parietal lobule; SPL, superior parietal lobule; CUN, cuneus; PCUN, precuneus; pre-SMA, pre-supplementary motor area; FUS, fusiform gyrus.

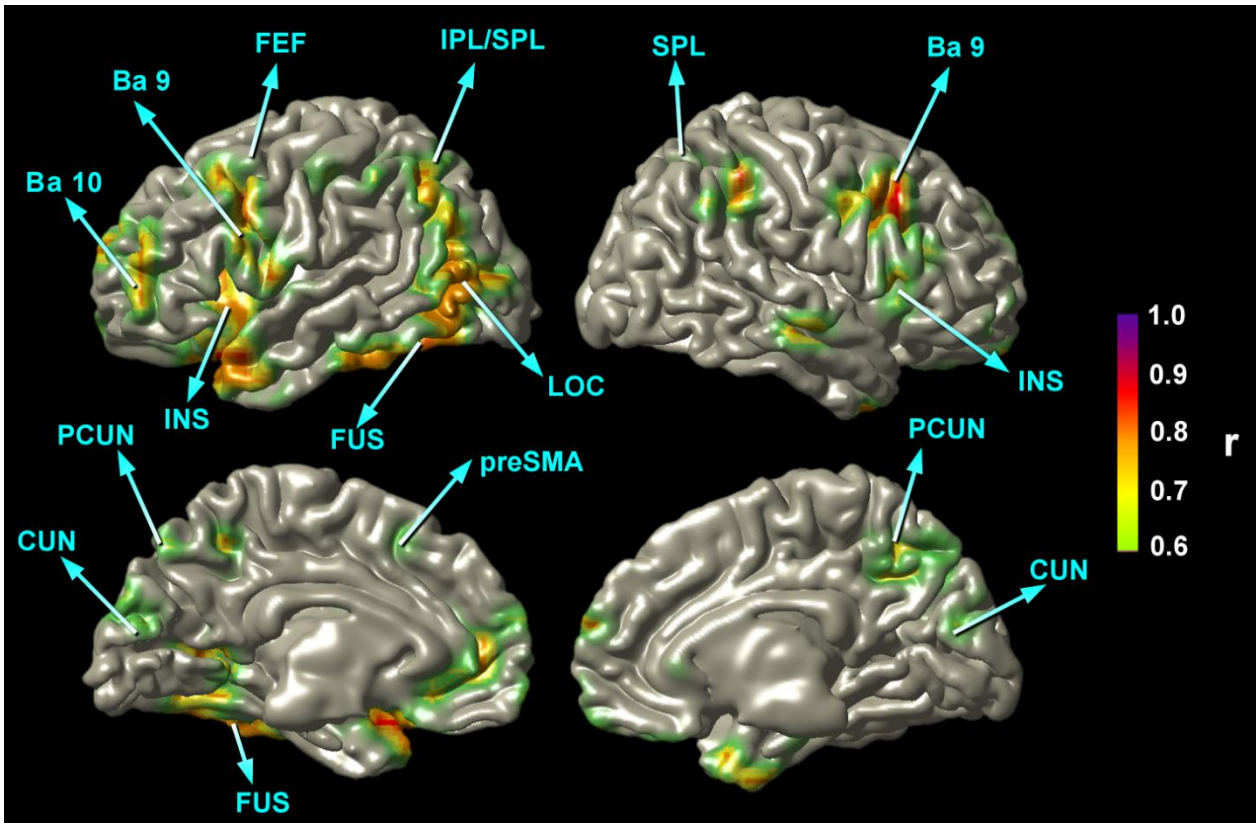

Figure 4.3 MEG neural activity correlated with performance

Neural activity from MEG experiment correlated with performance across subjects for *object* change conditions. Correlations are significant at $p < 0.05$. Labeled regions: Ba 10, Brodmann area 10; Ba 9, Brodmann area 9; FEF, frontal eye field; IPL, inferior parietal lobule; SPL, superior parietal lobule; CUN, cuneus; PCUN, precuneus; pre-SMA, pre-supplementary motor area; FUS, fusiform gyrus..

Activity which correlated with behavioral performance produced a similar profile using both fMRI and MEG methods. Specifically, the results revealed the fronto-parietal network frequently implicated in working memory tasks (for review see Wager & Smith 2003). Moreover, clusters of voxels correlating with performance across both MEG and fMRI were observed in brain regions previously implicated in VWM tasks including the insula (e.g., Borowsky et al., 2005; Todd et al., 2011), fusiform gyrus (e.g., Courtney et al., 1996; Ungerleider et al., 1998), cuneus and precuneus (e.g., Sala & Courtney, 2007), pre-SMA

(e.g., Petit et al., 1998), left FEF (e.g., Harrison et al., 2010; Mohr et al., 2006), LOC (e.g., Todd & Marois, 2004; Xu & Chun, 2006), and Ba 10 (e.g., Sala et al., 2003). These results suggest that while both imaging techniques measure different aspects of brain activation, there exists overlap in the detection of activity within specific brain regions, particularly in the context of VWM. Specifically, the ERD in the theta range appears to increase as performance increases in all regions which overlap with the correlated fMRI clusters except for the pre-SMA and the left Ba 10. In those two regions, increases in ERS correlates with increased performance providing an analogous positive correlation with the one observed within the fMRI experiment.

An fMRI study by Klingberg et al. (2002) identified the left FEF and IPL as regions which demonstrated a positive correlation with WM performance (memory capacity). A similar VWM study by Linden et al. (2003) found a positive correlation between behavioral performance and the BOLD response in the left DLPFC and the pre-SMA bilaterally. Together, these two studies suggest a performance-based functional network corresponding to a fronto-parietal network as well as the left FEF and pre-SMA. Accordingly, our findings are in agreement with this network across both fMRI recordings and the localization of the theta band of recorded MEG signals.

Results from both fMRI and MEG experiments in conjunction with the correlational analysis described above reveal several findings. First, both MEG and fMRI measure similar profiles of activation corresponding to VWM. While this point may not be apparent in the fMRI and MEG results of individual CD

conditions, when correlated with behavioral performance, a similar network of brain regions emerges. Second, condition effects observed across object and location conditions for both fMRI and MEG suggests a caudal-rostral model of location-object dissociation. If the results from previous fMRI studies, which attempted to dissociate object and location memory, are interpreted within the context of a caudal-rostral model, then concordant results suggestive of such a model emerge. Therefore, this study provides novel evidence in support of domain-based memory segregation while also reporting results which are in agreement with previous fMRI studies. Moreover, these findings may be aid in disambiguating deficits associated with working memory which have been previously identified within specific patient populations including Alzheimer's disease (e.g., Carlesimo & Oscar-Berman, 1992; Kaszniak, 1986), mild traumatic brain injury (mTBI) (e.g., Jantzen et al., 2004; McAllister et al., 2001), autism (e.g., Steele et al., 2007; Williams et al., 2006), depression (e.g., Christopher & MacDonald, 2005; Rose & Ebmeier, 2005), schizophrenia (e.g., Gold et al., 1992; Walter et al., 2007), post-traumatic stress disorder (PTSD) (e.g., Galletly et al., 2001; Weber et al., 2005), and multiple sclerosis (MS) (e.g., Covey et al., 2011; Litvan et al., 1988).

The limitations of the present study are not a reflection of the study design but rather an issue with participant recruitment and analysis methods. While ten subjects were recruited for each CD condition across both fMRI and MEG acquisitions, the cohort for each modality and condition varied slightly. This was due to MEG scanning restrictions for certain subjects in regards to metal artifacts

(i.e., permanent retainer) and delays in between fMRI and MEG scans for certain subjects who were not available at later points. An identical cohort of participants across techniques may have provided more robust results across object and location memory conditions and imaging modalities. Additionally, a larger sample of subjects for each WM condition would have allowed for more degrees of freedom in the data analyses, possibly yielding additional loci of object-location dissociation. Moreover, this sample contained a relatively narrow age range (23-33 years old), which may have restricted the interpretation of these findings to a younger age demographic rather than allowing for a general interpretation across all age ranges. In regards to analysis methods, different software suites between fMRI and MEG methods precluded the possibility of mapping source localization in a unitary model although sources were reported in a uniform source space (Talairach coordinate system) across imaging modalities. By utilizing a single source model for both modalities, a direct comparison on a voxel-by-voxel basis of MEG and fMRI data would have been possible to determine the loci of correlated activity across techniques.

4.2 Future Directions

Characterizing the activity associated with object and location memory in fMRI and MEG provides a foundation upon which additional parameters of WM may be explored. For example, while WM workload has been explored in detail using fMRI (e.g., Todd & Marois, 2004), EEG (e.g., Vogel & Machizawa, 2004), and MEG (e.g., Robitaille et al., 2009), it has not been studied within the context of object and location WM. Studies employing a similar CD paradigm as the one

described here could further elucidate the brain regions responsible for increased location memory as compared to object identity memory. While a recent study by Harrison et al. (2010) has explored workload within each of these memory domains, items were presented in a serial manner which added an unaccounted for temporal component to the design. Furthermore, the task was limited to fMRI only.

In addition to studying object and location WM, a third component, time, may be studied in future experiments. The order in which stimuli are presented plays an important role in WM especially in the context of proactive interference (PI) (e.g., Shiffrin & Atkinson, 1969). Tasks similar to the one employed in this study may be modified to identify brain regions associated with items viewed in previous trials over long or short delays. This time parameter may also be explored within the context of object and location memory such that divergent functional networks correspond to the time associated with remembering specific objects as compared to remembering specific locations.

4.3 Conclusions

The studies presented in this dissertation have provided evidence that maintenance of VWM for object identities and locations follow a caudal-rostral rather than a dorsal-ventral direction. Furthermore, while multiple challenges associated with comparing imaging modalities exist, this study provides the first evidence of convergent VWM results across techniques. While findings from both fMRI and MEG experiments did not produce a functional dissociation following a

prefrontal dorsal-ventral separation, a general caudal-rostral dissociation was observed. The proposed caudal-rostral interpretation of location and object identity memory provides a novel context within which to explore the neural substrates of WM across imaging techniques and populations.

BIBLIOGRAPHY

1. Allison T, McCarthy G, Nobre A, Puce A, Belger A. Human extrastriate visual cortex and the perception of faces, words, numbers, and colors. Cereb Cortex. 1994 Sep-Oct;4(5):544-54. Review.

2. Asada H, Fukuda Y, Tsunoda S, Yamaguchi M, Tonoike M. Frontal midline theta rhythms reflect alternative activation of prefrontal cortex and anterior cingulate cortex in humans. Neurosci Lett. 1999 Oct 15;274(1):29-32.

3. Bachevalier J, Mishkin M. Visual recognition impairment follows ventromedial but not dorsolateral prefrontal lesions in monkeys. Behav Brain Res. 1986 Jun;20(3):249-61.

4. Baddeley A, Hitch G. Working memory. In: Bower GH, editor. The psychology of learning and motivation: advances in research and theory. New York: Academic Press. 1974. pp. 47–8.

5. Baddeley A, Logie R, Bressi S, Della Sala S, Spinnler H. Dementia and working memory. Q J Exp Psychol A. 1986 Nov;38(4):603-18.

6. Bandettini PA, Wong EC, Hinks RS, Tikofsky RS, Hyde JS. Time course EPI of human brain function during task activation. Magn Reson Med. 1992Jun;25(2):390-7.

7. Bastiaansen MC, Posthuma D, Groot PF, de Geus EJ. Event-related alpha and theta responses in a visuo-spatial working memory task. Clin Neurophysiol. 2002Dec;113(12):1882-93.

8. Borowsky R, Loehr J, Kelland Friesen C, Kraushaar G, Kingstone A, Sarty G. Modularity and intersection of "what", "where" and "how" processing of visual stimuli: a new method of FMRI localization. Brain Topogr. 2005 Winter;18(2):67-

75.

9. Brookes MJ, Wood JR, Stevenson CM, Zumer JM, White TP, Liddle PF, Morris PG. Changes in brain network activity during working memory tasks: a magnetoencephalography study. Neuroimage. 2011 Apr 15;55(4):1804-15.

10. Cabeza R, Nyberg L. Imaging cognition II: An empirical review of 275 PET and fMRI studies. J Cogn Neurosci. 2000 Jan;12(1):1-47. Review.

11. Callan D, Callan A, Gamez M, Sato MA, Kawato M. Premotor cortex mediates perceptual performance. Neuroimage. 2010 Jun;51(2):844-58.

12. Campo P, Maestú F, Ortiz T, Capilla A, Santiuste M, Fernández A, Amo C. Time modulated prefrontal and parietal activity during the maintenance of integrated information as revealed by magnetoencephalography. Cereb Cortex. 2005 Feb;15(2):123-30

13. Carlesimo GA, Oscar-Berman M. Memory deficits in Alzheimer's patients: a comprehensive review. Neuropsychol Rev. 1992 Jun;3(2):119-69. Review.

14. Christopher G, MacDonald J. The impact of clinical depression on working memory. Cogn Neuropsychiatry. 2005 Nov;10(5):379-99.

15. Cichy RM, Chen Y, Haynes JD. Encoding the identity and location of objects in human LOC. Neuroimage. 2011 Feb 1;54(3):2297-307.

16. Ciesielski KT, Ahlfors SP, Bedrick EJ, Kerwin AA, Hämäläinen MS. Top-down control of MEG alpha-band activity in children performing Categorical N-Back Task. Neuropsychologia. 2010 Oct;48(12):3573-9.

17. Clark VP, Keil K, Maisog JM, Courtney S, Ungerleider LG, Haxby JV. Functional magnetic resonance imaging of human visual cortex during face

matching: a comparison with positron emission tomography. Neuroimage. 1996 Aug;4(1):1-15.

18. Cohen JD, Perlstein WM, Braver TS, Nystrom LE, Noll DC, Jonides J, Smith EE. Temporal dynamics of brain activation during a working memory task. Nature. 1997 Apr 10;386(6625):604-8.

19. Courtney SM, Petit L, Maisog JM, Ungerleider LG, Haxby JV. An area specialized for spatial working memory in human frontal cortex. Science. 1998 Feb27;279(5355):1347-51.

20. Courtney SM, Ungerleider LG, Keil K, Haxby JV. Object and spatial visual working memory activate separate neural systems in human cortex. Cereb Cortex. 1996 Jan-Feb;6(1):39-49.

21. Courtney SM, Ungerleider LG, Keil K, Haxby JV. Transient and sustained activity in a distributed neural system for human working memory. Nature. 1997 Apr 10;386(6625):608-11.

22. Covey TJ, Zivadinov R, Shucard JL, Shucard DW. Information processing speed, neural efficiency, and working memory performance in multiple sclerosis: Differential relationships with structural magnetic resonance imaging. J Clin Exp Neuropsychol. 2011 Nov 3.

23. Cox RW. AFNI: software for analysis and visualization of functional magnetic resonance neuroimages. Comput Biomed Res. 1996 Jun;29(3):162-73.

24. Curtis CE, D'Esposito M. Persistent activity in the prefrontal cortex during working memory. Trends Cogn Sci. 2003 Sep;7(9):415-423.

25. Damoiseaux JS, Rombouts SA, Barkhof F, Scheltens P, Stam CJ, Smith

SM, Beckmann CF. Consistent resting-state networks across healthy subjects. Proc Natl Acad Sci U S A. 2006 Sep 12;103(37):13848-53.

26. Desimone R, Ungedeider LG. Neural mechanisms of visual processing in monkeys. In Handbook of Neuropsychology, Vol.2, ed. F Boller, J Grafman. New York: Elsevier. 1989. pp. 267-99.

27. D'Esposito M, Aguirre GK, Zarahn E, Ballard D, Shin RK, Lease J. Functional MRI studies of spatial and nonspatial working memory. Brain Res Cogn Brain Res. 1998 Jul;7(1):1-13.

28. Doppelmayr M, Klimesch W, Schwaiger J, Auinger P, Winkler T. Theta synchronization in the human EEG and episodic retrieval. Neurosci Lett. 1998 Nov20;257(1):41-4.

29. Duncan J, Owen AM. Common regions of the human frontal lobe recruited by diverse cognitive demands. Trends Neurosci. 2000 Oct;23(10):475-83. Review.

30. Düzel E, Habib R, Schott B, Schoenfeld A, Lobaugh N, McIntosh AR, Scholz M, Heinze HJ. A multivariate, spatiotemporal analysis of electromagnetic time-frequency data of recognition memory. Neuroimage. 2003 Feb;18(2):185-97.

31. Ettlinger G. "Object vision" and "spatial vision": the neuropsychological evidence for the distinction. Cortex. 1990 Sep;26(3):319-41. Review.

32. Fox PT, Fox JM, Raichle ME, Burde RM. The role of cerebral cortex in the generation of voluntary saccades: a positron emission tomographic study. J Neurophysiol. 1985 Aug;54(2):348-69.

33. Frisk V, Milner B. The relationship of working memory to the immediate recall of stories following unilateral temporal or frontal lobectomy. Neuropsychologia. 1990;28(2):121-35.

34. Funahashi S, Bruce CJ, Goldman-Rakic PS. Dorsolateral prefrontal lesions and oculomotor delayed-response performance: evidence for mnemonic "scotomas". J Neurosci. 1993 Apr;13(4):1479-97.

35. Funahashi S, Bruce CJ, Goldman-Rakic PS. Mnemonic coding of visual space in the monkey's dorsolateral prefrontal cortex. J Neurophysiol. 1989Feb;61(2):331-49.

36. G lezer LS, Jiang X, Riesenhuber M. Evidence for highly selective neuronal tuning to whole words in the "visual word form area". Neuron. 2009 Apr30;62(2):199-204.

37. Gaetz W, Edgar JC, Wang DJ, Roberts TP. Relating MEG measured motor cortical oscillations to resting γ-aminobutyric acid (GABA) concentration. Neuroimage. 2011 Mar 15;55(2):616-21.

38. Galletly C, Clark CR, McFarlane AC, Weber DL. Working memory in post traumaticstress disorder--an event-related potential study. J Trauma Stress. 2001Apr;14(2):295-309.

39. Gold JM, Randolph C, Carpenter CJ, Goldberg TE, Weinberger DR. Forms of memory failure in schizophrenia. J Abnorm Psychol. 1992 Aug;101(3):487-94.

40. Gonçalves SI, de Munck JC, Pouwels PJ, Schoonhoven R, Kuijer JP, Maurits NM, Hoogduin JM, Van Someren EJ, Heethaar RM, Lopes da Silva FH. Correlating the alpha rhythm to BOLD using simultaneous EEG/fMRI: inter-

subject variability. Neuroimage. 2006 Mar;30(1):203-13.

41. Grill-Spector K. The neural basis of object perception. Curr Opin Neurobiol. 2003 Apr;13(2):159-66. Review. Erratum in: Curr Opin Neurobiol. 2003 Jun;13(3):399.

42. Grimault S, Robitaille N, Grova C, Lina JM, Dubarry AS, Jolicoeur P. Oscillatory activity in parietal and dorsolateral prefrontal cortex during retention in visual short-term memory: additive effects of spatial attention andmemory load. Hum Brain Mapp. 2009 Oct;30(10):3378-92.

43. Gross J, Kujala J, Hamalainen M, Timmermann L, Schnitzler A, Salmelin R. Dynamic imaging of coherent sources: Studying neural interactions in the human brain. Proc Natl Acad Sci U S A. 2001 Jan 16;98(2):694-9.

44. Harrison A, Jolicoeur P, Marois R. "What" and "where" in the intraparietal sulcus: an FMRI study of object identity and location in visual short-term memory. Cereb Cortex. 2010 Oct;20(10):2478-85.

45. Haxby JV, Horwitz B, Ungerleider LG, Maisog JM, Pietrini P, Grady CL. The functional organization of human extrastriate cortex: a PET-rCBF study of selective attention to faces and locations. J Neurosci. 1994 Nov;14(11 Pt1):6336-53.

46. Haxby JV, Petit L, Ungerleider LG, Courtney SM. Distinguishing the functional roles of multiple regions in distributed neural systems for visual working memory. Neuroimage. 2000 Feb;11(2):145-56.

47. Hirata M, Goto T, Barnes G, Umekawa Y, Yanagisawa T, Kato A, Oshino S, Kishima H, Hashimoto N, Saitoh Y, Tani N, Yorifuji S, Yoshimine T. Language

dominance and mapping based on neuromagnetic oscillatory changes: comparison with invasive procedures. J Neurosurg. 2010 Mar;112(3):528-38.

48. Hocking J, Price CJ. Dissociating verbal and nonverbal audiovisual object processing. Brain Lang. 2009 Feb;108(2):89-96.

49. Ishii R, Shinosaki K, Ukai S, Inouye T, Ishihara T, Yoshimine T, Hirabuki N, Asada H, Kihara T, Robinson SE, Takeda M. Medial prefrontal cortex generates frontal midline theta rhythm. Neuroreport. 1999 Mar 17;10(4):675-9.

50. James TW, Culham J, Humphrey GK, Milner AD, Goodale MA. Ventral occipital lesions impair object recognition but not object-directed grasping: an fMRI study. Brain. 2003 Nov;126(Pt 11):2463-75.

51. Jantzen KJ, Anderson B, Steinberg FL, Kelso JA. A prospective functional MR imaging study of mild traumatic brain injury in college football players. AJNR Am J Neuroradiol. 2004 May;25(5):738-45.

52. Jensen O, Tesche CD. Frontal theta activity in humans increases with memory load in a working memory task. Eur J Neurosci. 2002 Apr;15(8):1395-9.

53. Jokisch D, Jensen O. Modulation of gamma and alpha activity during a working memory task engaging the dorsal or ventral stream. J Neurosci. 2007 Mar 21;27(12):3244-51.

54. Jonides J, Smith EE, Koeppe RA, Awh E, Minoshima S, Mintun MA. Spatial working memory in humans as revealed by PET. Nature. 1993 Jun 17;363(6430):623-5.

55. Kaszniak AW, Wilson RS, Fox JH, Stebbins GT. Cognitive assessment in Alzheimer's disease: cross-sectional and longitudinal perspectives. Can J Neurol

Sci. 1986 Nov;13(4 Suppl):420-3.

56. Khursheed F, Tandon N, Tertel K, Pieters TA, Disano MA, Ellmore TM. Frequency-specific electrocorticographic correlates of working memory delay period fMRI activity. Neuroimage. 2011 Jun 1;56(3):1773-82.

57. Kikuchi M, Shitamichi K, Ueno S, Yoshimura Y, Remijn GB, Nagao K, Munesue T, Iiyama K, Tsubokawa T, Haruta Y, Inoue Y, Watanabe K, Hashimoto T, Higashida H, Minabe Y. Neurovascular coupling in the human somatosensory cortex: a single trial study. Neuroreport. 2010 Dec 8;21(17):1106-10.

58. Klimesch W, Doppelmayr M, Pachinger T, Ripper B. Brain oscillations and human memory: EEG correlates in the upper alpha and theta band. Neurosci Lett. 1997 Nov 28;238(1-2):9-12.

59. Köhler S, Moscovitch M, Winocur G, Houle S, McIntosh AR. Networks of domain-specific and general regions involved in episodic memory for spatial location and object identity. Neuropsychologia. 1998 Feb;36(2):129-42.

60. Krause CM, Sillanmäki L, Koivisto M, Saarela C, Häggqvist A, Laine M, Hämäläinen H. The effects of memory load on event-related EEG desynchronization and synchronization. Clin Neurophysiol. 2000 Nov;111(11):2071-8.

61. Kravitz DJ, Vinson LD, Baker CI. How position dependent is visual object recognition? Trends Cogn Sci. 2008 Mar;12(3):114-22. Review.

62. Lange KW, Sahakian BJ, Quinn NP, Marsden CD, Robbins TW. Comparison of executive and visuospatial memory function in Huntington's disease and dementia of Alzheimer type matched for degree of dementia. J

Neurol Neurosurg Psychiatry. 1995 May;58(5):598-606.

63. Leung AW, Alain C. Working memory load modulates the auditory "What" and "Where" neural networks. Neuroimage. 2011 Apr 1;55(3):1260-9.

64. Levy R, Goldman-Rakic PS. Association of storage and processing functions in the dorsolateral prefrontal cortex of the nonhuman primate. J Neurosci. 1999 Jun15;19(12):5149-58.

65. Levy R, Goldman-Rakic PS. Segregation of working memory functions within the dorsolateral prefrontal cortex. Exp Brain Res. 2000 Jul;133(1):23-32. Review.

66. Li L, Zhang JX, Jiang T. Visual working memory load-related changes in neural activity and functional connectivity. PLoS One. 2011;6(7):e22357.

67. Linden DE, Bittner RA, Muckli L, Waltz JA, Kriegeskorte N, Goebel R, Singer W, Munk MH. Cortical capacity constraints for visual working memory: dissociation of fMRI load effects in a fronto-parietal network. Neuroimage. 2003 Nov;20(3):1518-30.

68. Litvan I, Grafman J, Vendrell P, Martinez JM, Junqué C, Vendrell JM, Barraquer-Bordas JL. Multiple memory deficits in patients with multiple sclerosis. Exploring the working memory system. Arch Neurol. 1988 Jun;45(6):607-10.

69. Livingstone MS, Hubel DH. Psychophysical evidence for separate channels for the perception of form, color, movement, and depth. J Neurosci. 1987 Nov;7(11):3416-68. Review.

70. Logothetis NK. The neural basis of the blood-oxygen-level-dependent functional magnetic resonance imaging signal. Philos Trans R Soc Lond B Biol

Sci. 2002 Aug29;357(1424):1003-37. Review.

71. Ma L, Jiang Y, Bai J, Gong Q, Liu H, Chen HC, He S, Weng X. Robust and task-independent spatial profile of the visual word form activation in fusiform cortex. PLoS One. 2011;6(10):e26310.

72. Macko, K. A. et al. Mapping the primate visual system with [2–14C] deoxyglucose. Science 218, 394–397 (1982).

73. Malach R, Reppas JB, Benson RR, Kwong KK, Jiang H, Kennedy WA, Ledden PJ, Brady TJ, Rosen BR, Tootell RB. Object-related activity revealed by functional magnetic resonance imaging in human occipital cortex. Proc Natl Acad Sci U S A. 1995 Aug 29;92(18):8135-9.

74. McAllister TW, Sparling MB, Flashman LA, Saykin AJ. Neuroimaging findings in mild traumatic brain injury. J Clin Exp Neuropsychol. 2001 Dec;23(6):775-91. Review.

75. McCarthy G, Puce A, Constable RT, Krystal JH, Gore JC, Goldman-Rakic P. Activation of human prefrontal cortex during spatial and nonspatial working memory tasks measured by functional MRI. Cereb Cortex. 1996 Jul-Aug;6(4):600-11.

76. Meltzer JA, Zaveri HP, Goncharova II, Distasio MM, Papademetris X, Spencer SS, Spencer DD, Constable RT. Effects of working memory load on oscillatory power in human intracranial EEG. Cereb Cortex. 2008 Aug;18(8):1843-55.

77. Michels L, Bucher K, Lüchinger R, Klaver P, Martin E, Jeanmonod D, Brandeis D. Simultaneous EEG-fMRI during a working memory task: modulations

in low and high frequency bands. PLoS One. 2010 Apr 22;5(4):e10298.

78. Miller EK, Cohen JD. An integrative theory of prefrontal cortex function. Annu Rev Neurosci. 2001;24:167-202. Review.

79. Milner AD, Perrett DI, Johnston RS, Benson PJ, Jordan TR, Heeley DW, Bettucci D, Mortara F, Mutani R, Terazzi E, et al. Perception and action in 'visual form agnosia'. Brain. 1991 Feb;114 (Pt 1B):405-28.

80. Mishkin, M., Ungerleider, L.G., & Macko, K.A. Object vision and spatial vision: two cortical pathways. Trends in Neuroscience. 1983; 6:414- 417.

81. Mizuhara H, Yamaguchi Y. Neuronal ensemble for visual working memory via interplay of slow and fast oscillations. Eur J Neurosci. 2011 May;33(10):1925-34.

82. Mohr HM, Goebel R, Linden DE. Content- and task-specific dissociations of frontal activity during maintenance and manipulation in visual working memory. J Neurosci. 2006 Apr 26;26(17):4465-71.

83. Morris RG, Gick ML, Craik FI. Processing resources and age differences in working memory. Mem Cognit. 1988 Jul;16(4):362-6.

84. Moscovitch C, Kapur S, Köhler S, Houle S. Distinct neural correlates of visual long-term memory for spatial location and object identity: a positron emission tomography study in humans. Proc Natl Acad Sci U S A. 1995 Apr 25;92(9):3721-5.

85. Moses SN, Bardouille T, Brown TM, Ross B, McIntosh AR. Learning related activation of somatosensory cortex by an auditory stimulus recorded with magnetoencephalography. Neuroimage. 2010 Oct 15;53(1):275-82.

86. Mottaghy FM, Döring T, Müller-Gärtner HW, Töpper R, Krause BJ. Bilateral parieto-frontal network for verbal working memory: an interference approach using repetitive transcranial magnetic stimulation (rTMS). Eur J Neurosci. 2002 Oct;16(8):1627-32.

87. Müller NG, Knight RT. The functional neuroanatomy of working memory: contributions of human brain lesion studies. Neuroscience. 2006 Apr28;139(1):51-8.

88. Munk MH, Linden DE, Muckli L, Lanfermann H, Zanella FE, Singer W, Goebel R. Distributed cortical systems in visual short-term memory revealed by event-related functional magnetic resonance imaging. Cereb Cortex. 2002Aug;12(8):866-76.

89. Olesen PJ, Nagy Z, Westerberg H, Klingberg T. Combined analysis of DTI and fMRI data reveals a joint maturation of white and grey matter in a fronto-parietal network. Brain Res Cogn Brain Res. 2003 Dec;18(1):48-57.

90. Onton J, Delorme A, Makeig S. Frontal midline EEG dynamics during working memory. Neuroimage. 2005 Aug 15;27(2):341-56.

91. Op de Beeck HP, Dicarlo JJ, Goense JB, Grill-Spector K, Papanastassiou A, Tanifuji M, Tsao DY. Fine-scale spatial organization of face and object selectivity in the temporal lobe: do functional magnetic resonance imaging, optical imaging, and electrophysiology agree? J Neurosci. 2008 Nov12;28(46):11796-801. Review.

92. Owen AM, Downes JJ, Sahakian BJ, Polkey CE, Robbins TW. Planning and spatial working memory following frontal lobe lesions in man.

Neuropsychologia. 1990;28(10):1021-34.

93. Owen AM, Herrod NJ, Menon DK, Clark JC, Downey SP, Carpenter TA, Minhas PS, Turkheimer FE, Williams EJ, Robbins TW, Sahakian BJ, Petrides M, Pickard JD. Redefining the functional organization of working memory processes within human lateral prefrontal cortex. Eur J Neurosci. 1999 Feb;11(2):567-74.

94. Owen AM. The role of the lateral frontal cortex in mnemonic processing: the contribution of functional neuroimaging. Exp Brain Res. 2000 Jul;133(1):33-43.Review.

95. Palva S, Monto S, Palva JM. Graph properties of synchronized cortical networks during visual working memory maintenance. Neuroimage. 2010 Feb 15;49(4):3257-68.

96. Papanicolaou AC, Simos PG, Breier JI, Zouridakis G, Willmore LJ, Wheless JW, Constantinou JE, Maggio WW, Gormley WB. Magnetoencephalographic mapping of the language-specific cortex. J Neurosurg. 1999 Jan;90(1):85-93.

97. Park S, Holzman PS. Schizophrenics show spatial working memory deficits. Arch Gen Psychiatry. 1992 Dec;49(12):975-82.

98. Passaro AD, Rezaie R, Moser DC, Li Z, Dias N, Papanicolaou AC. Optimizing estimation of hemispheric dominance for language using magnetic source imaging. Brain Res. 2011 Oct 6;1416:44-50.

99. Passingham RE. Memory of monkeys (Macaca mulatta) with lesions in prefrontal cortex. Behav Neurosci. 1985 Feb;99(1):3-21.

100. Pazo-Alvarez P, Simos PG, Castillo EM, Juranek J, Passaro AD,

Papanicolaou AC. MEG correlates of bimodal encoding of faces and persons' names. Brain Res. 2008Sep 16;1230:192-201.

101. Pessoa L, Gutierrez E, Bandettini P, Ungerleider L. Neural correlates of visual working memory: fMRI amplitude predicts task performance. Neuron. 2002 Aug29;35(5):975-87.

102. Petit L, Courtney SM, Ungerleider LG, Haxby JV. Sustained activity in the medial wall during working memory delays. J Neurosci. 1998 Nov 15;18(22):9429-37.

103. Petrides M, Alivisatos B, Evans AC, Meyer E. Dissociation of human mid-dorsolateral from posterior dorsolateral frontal cortex in memory processing. Proc Natl Acad Sci U S A. 1993 Feb 1;90(3):873-7.

104. Petrides M. Impairments on nonspatial self-ordered and externally ordered working memory tasks after lesions of the mid-dorsal part of the lateral frontal cortex in the monkey. J Neurosci. 1995 Jan;15(1 Pt 1):359-75.

105. Petrides M. Lateral prefrontal cortex: architectonic and functional organization. Philos Trans R Soc Lond B Biol Sci. 2005 Apr 29;360(1456):781-95. Review.

106. Pisella L, Berberovic N, Mattingley JB. Impaired working memory for location but not for colour or shape in visual neglect: a comparison of parietal and non-parietal lesions. Cortex. 2004 Apr;40(2):379-90.

107. Posner MI, Konick AF. On the role of interference in short-term retention. J Exp Psychol. 1966 Aug;72(2):221-31.

108. Postle BR, D'Esposito M. "What"-Then-Where" in visual working memory:

an event-related fMRI study. J Cogn Neurosci. 1999 Nov;11(6):585-97.

109. Postle BR, Stern CE, Rosen BR, Corkin S. An fMRI investigation of cortical contributions to spatial and nonspatial visual working memory. Neuroimage. 2000 May;11(5 Pt 1):409-23.

110. Puce A, Allison T, Gore JC, McCarthy G. Face-sensitive regions in human extrastriate cortex studied by functional MRI. J Neurophysiol. 1995Sep;74(3):1192-9.

111. Raghavachari S, Kahana MJ, Rizzuto DS, Caplan JB, Kirschen MP, Bourgeois B, Madsen JR, Lisman JE. Gating of human theta oscillations by a working memory task. J Neurosci. 2001 May 1;21(9):3175-83.

112. Rämä P, Poremba A, Sala JB, Yee L, Malloy M, Mishkin M, Courtney SM. Dissociable functional cortical topographies for working memory maintenance of voice identity and location. Cereb Cortex. 2004 Jul;14(7):768-80.

113. Robitaille N, Grimault S, Jolicoeur P. Bilateral parietal and contralateral responses during maintenance of unilaterally encoded objects in visual short-term memory: evidence from magnetoencephalography. Psychophysiology. 2009Sep;46(5):1090-9.

114. Rose EJ, Ebmeier KP. Pattern of impaired working memory during major depression. J Affect Disord. 2006 Feb;90(2-3):149-61.

115. Rossion B, Dricot L, Devolder A, Bodart JM, Crommelinck M, De Gelder B, Zoontjes R. Hemispheric asymmetries for whole-based and part-based face processing in the human fusiform gyrus. J Cogn Neurosci. 2000 Sep;12(5):793-802.

116. Rushworth MF, Nixon PD, Eacott MJ, Passingham RE. Ventral prefrontal cortex is not essential for working memory. J Neurosci. 1997 Jun 15;17(12):4829-38.

117. Rutkowski JS, Crewther DP, Crewther SG. Change detection is impaired in children with dyslexia. J Vis. 2003;3(1):95-105.

118. Saad ZS, Glen DR, Chen G, Beauchamp MS, Desai R, Cox RW. A new method for improving functional-to-structural MRI alignment using local Pearson correlation. Neuroimage. 2009 Feb 1;44(3):839-48.

119. Sala JB, Courtney SM. Binding of what and where during working memory maintenance. Cortex. 2007 Jan;43(1):5-21.

120. Sala JB, Rämä P, Courtney SM. Functional topography of a distributed neural system for spatial and nonspatial information maintenance in working memory. Neuropsychologia. 2003;41(3):341-56.

121. Sarvas J. Basic mathematical and electromagnetic concepts of the biomagnetic inverse problem. Phys Med Biol. 1987 Jan;32(1):11-22.

122. Scheeringa R, Petersson KM, Oostenveld R, Norris DG, Hagoort P, Bastiaansen MC. Trial-by-trial coupling between EEG and BOLD identifies networks related to alpha and theta EEG power increases during working memory maintenance. Neuroimage. 2009 Feb 1;44(3):1224-38.

123. Seeley WW, Menon V, Schatzberg AF, Keller J, Glover GH, Kenna H, Reiss AL, Greicius MD. Dissociable intrinsic connectivity networks for salience processing and executive control. J Neurosci. 2007 Feb 28;27(9):2349-56.

124. Sergent J, Ohta S, MacDonald B. Functional neuroanatomy of face and

object processing. A positron emission tomography study. Brain. 1992 Feb;115 Pt 1:15-36.

125. Shen L, Hu X, Yacoub E, Ugurbil K. Neural correlates of visual form and visual spatial processing. Hum Brain Mapp. 1999;8(1):60-71.

126. Shiffrin RM, Atkinson RC. Storage and retrieval processes in long-term memory. Psychological Review. 1969;76:179–193.

127. Simos PG, Papanicolaou AC, Breier JI, Fletcher JM, Wheless JW, Maggio WW, Gormley W, Constantinou JE, Kramer L. Insights into brain function and neural plasticity using magnetic source imaging. J Clin Neurophysiol. 2000Mar;17(2):143-62. Review.

128. Smith EE, Jonides J, Koeppe RA, Awh E, Schumacher EH, Minoshima S. Spatial versus object working memory: PET investigations. J Cogn Neurosci. 1995 7:337–356.

129. Smith EE, Jonides J, Koeppe RA. Dissociating verbal and spatial working memory using PET. Cereb Cortex. 1996 Jan-Feb;6(1):11-20. Erratum in: Cereb Cortex 1998Dec;8(8):762.

130. Smith EE, Jonides J. Neuroimaging analyses of human working memory. Proc Natl Acad Sci U S A. 1998 Sep 29;95(20):12061-8. Review.

131. Smith EE, Jonides J. Storage and executive processes in the frontal lobes. Science. 1999 Mar 12;283(5408):1657-61. Review.

132. Smith EE, Jonides J. Working memory: a view from neuroimaging. Cogn Psychol. 1997 Jun;33(1):5-42. Review.

133. Steele SD, Minshew NJ, Luna B, Sweeney JA. Spatial working memory

deficits in autism. J Autism Dev Disord. 2007 Apr;37(4):605-12.

134. Stevenson CM, Wang F, Brookes MJ, Zumer JM, Francis ST, Morris PG. Paired pulse depression in the somatosensory cortex: Associations between MEG and BOLD fMRI. Neuroimage. 2011 Oct 20.

135. Stuss DT, Levine B. Adult clinical neuropsychology: lessons from studies of the frontal lobes. Annu Rev Psychol. 2002;53:401-33. Review.

136. Tavabi K, Embick D, Roberts TP. Word repetition priming-induced oscillations in auditory cortex: a magnetoencephalography study. Neuroreport. 2011 Dec7;22(17):887-91.

137. Todd JJ, Han SW, Harrison S, Marois R. The neural correlates of visual working memory encoding: a time-resolved fMRI study. Neuropsychologia. 2011May;49(6):1527-36.

138. Todd JJ, Marois R. Capacity limit of visual short-term memory in human posterior parietal cortex. Nature. 2004 Apr 15;428(6984):751-4.

139. Ungerleider LG, Courtney SM, Haxby JV. A neural system for human visual working memory. Proc Natl Acad Sci U S A. 1998 Feb 3;95(3):883-90. Review.

140. Ungerleider LG, Mishkin M. Two cortical visual systems. In DJ Ingle, MA Goodale, RJW Mansfield (Eds), Analysis of visual behavior. Cambridge,MA: MIT Press. 1982. pp. 549–586

141. Ungerleider LG. Functional brain imaging studies of cortical mechanisms for memory. Science. 1995 Nov 3;270(5237):769-75. Review.

142. Van Dijk H, van der Werf J, Mazaheri A, Medendorp WP, Jensen O.

Modulations in oscillatory activity with amplitude asymmetry can produce cognitively relevant event-related responses. Proc Natl Acad Sci U S A. 2010 Jan 12;107(2):900-5.

143. Vogel EK, Machizawa MG. Neural activity predicts individual differences in visual working memory capacity. Nature. 2004 Apr 15;428(6984):748-51.

144. Volle E, Kinkingnéhun S, Pochon JB, Mondon K, Thiebaut de Schotten M, Seassau M, Duffau H, Samson Y, Dubois B, Levy R. The functional architecture of the left posterior and lateral prefrontal cortex in humans. Cereb Cortex. 2008Oct;18(10):2460-9.

145. Wager TD, Smith EE. Neuroimaging studies of working memory: a meta-analysis. Cogn Affect Behav Neurosci. 2003 Dec;3(4):255-74. Review.

146. Walter H, Vasic N, Höse A, Spitzer M, Wolf RC. Working memory dysfunction in schizophrenia compared to healthy controls and patients with depression: evidence from event-related fMRI. Neuroimage. 2007 May 1;35(4):1551-61.

147. Weber DL, Clark CR, McFarlane AC, Moores KA, Morris P, Egan GF. Abnormal frontal and parietal activity during working memory updating in post-traumatic stress disorder. Psychiatry Res. 2005 Oct 30;140(1):27-44.

148. Westerberg H, Klingberg T. Changes in cortical activity after training of working memory--a single-subject analysis. Physiol Behav. 2007 Sep 10;92(1-2):186-92.

149. Willemse RB, de Munck JC, Verbunt JP, van 't Ent D, Ris P, Baayen JC, Stam CJ, Vandertop WP. Topographical organization of mu and Beta band

activity associated with hand and foot movements in patients with perirolandic lesions. Open Neuroimag J. 2010 Aug 2;4:93-9.

150. Williams DL, Goldstein G, Minshew NJ. The profile of memory function in children with autism. Neuropsychology. 2006 Jan;20(1):21-9.

151. Xu Y, Chun MM. Dissociable neural mechanisms supporting visual short-term memory for objects. Nature. 2006 Mar 2;440(7080):91-5.

152. Zumer JM, Brookes MJ, Stevenson CM, Francis ST, Morris PG. Relating BOLD fMRI and neural oscillations through convolution and optimal linear weighting. Neuroimage. 2010 Jan 15;49(2):1479-89.

VITA

Antony Passaro was born on October 9th, 1982, son of Paolo Passaro and Dr. Jane Chance. After graduating from St. Thomas Episcopal in 2001, he enrolled at Rice University in Houston, TX. There he received his Bachelor of Arts degree in cognitive sciences in 2005. After completing his undergraduate degree, he worked as a research assistant at the magnetoencephalography laboratory at the Center for Clinical Neurosciences at The University of Texas Health Science Center in Houston, TX. Antony enrolled as a graduate student in the Graduate School of Biomedical Sciences at The University of Texas Health Science Center at Houston in 2007.